AIIM

Association for Information and Image Management

1100 Wayne Avenue, Suite 1100
Silver Spring, Maryland 20910

301/587-8202

Centimeter

Inches

MANUFACTURED TO AIIM STANDARDS
BY APPLIED IMAGE, INC.

1 of 1

Collisional Stochastic Ripple Diffusion of Alpha Particles and Beam Ions on TFTR

M. H. Redi, M. C. Zarnstorff, R. B. White,

R. V. Budny, J. F. Schivell, S. D. Scott, S. J. Zweben

Princeton Plasma Physics Laboratory,

Princeton University, P. O. Box 451

Princeton, NJ 08543

Abstract

Predictions for ripple loss of fast ions from TFTR are investigated with a guiding center code including both collisional and ripple effects. Discrepancies between measurements and calculations of plasma beta at low current and large major radius are resolved when both effects are included for neutral beam ions. A synergistic enhancement of fast ion diffusion is found for toroidal field ripple with collisions. S = 5.4 for neutral beam ions and S = 1.4–2.4 for alpha particles. A 20–30% reduction in alpha particle heating is predicted for R = 2.6 m DT plasmas on TFTR due to first orbit and collisional stochastic ripple diffusion, although these losses will be reduced if q_a and R are smaller, as for most planned DT experiments.

MASTER

DISTRIBUTION OF THIS DOCUMENT IS UNLIMITED

1. Introduction

There has been considerable recent experimental and theoretical interest in the ripple and collisional loss of fast ions in high temperature tokamak fusion plasmas [1–24]. Because extensive computations which include both collisional and ripple loss processes are needed for useful predictions, efforts to include both effects for specific tokamak experiments have up to this point been limited to calculations for JT-60U [17]. Similar extensive computations [21–23] as well as approximate analytic treatments [6] have also been carried out for future reactors such as ITER and INTOR.

This is an important issue for the design of future tokamak reactors such as ITER because stochastic ripple diffusion of alpha particles deposits a strongly localized heat load on the first wall. Thus, in addition to clarifying questions about heat and particle transport, verification of code calculations of fast ion transport by comparison with experiment provides support for the design of future fusion devices. Here we carry out a detailed computational study for TFTR including both collisional and ripple transport effects for neutral beam ions in high q_a plasmas and for alpha particles in projected DT experiments.

Transport analysis of low current, full bore plasmas on TFTR has led to unexplained discrepanies between the measured and kinetically calculated stored plasma energies. The discrepancy in beta is found to increase with major radius and with reduced plasma current. The relatively poor performance of large major radius supershots at low Ip reflects this unexplained energy loss, which ranges from 10 to 40% of beta as calculated by the PPPL analysis codes SNAP [25] and TRANSP [26]. Standard SNAP and TRANSP analysis have not included ripple loss calculations. Clarification of this is particularly important for un-

derstanding ICRH plasma transport, since ICRH heating must be carried out on large bore plasmas for good antenna-plasma coupling. Low triton burnup measurements on TFTR, $1/2 \pm 1/4$ classical expectations [27], and also may be due to stochastic ripple loss.

Stochastic ripple losses were hypothesized to be responsible for the beta discrepancies by causing anomalously large losses of trapped neutral beam ions. Ripple losses of fast ions have been shown to cause significant losses on the ISX-B [11], JT-60U [17], JET [18, 19] and TORE SUPRA [20] tokamaks.

This simulation study is carried out with a Hamiltonian guiding center drift orbit code, ORBIT, developed by White and Chance [7], based on the canonical Hamiltonian guiding center variables of White [8]. Because of computational requirements only a few plasmas have been analysed with this method. These cases are intended to serve as benchmarks and guides in routine transport analysis, which will make use of faster, approximate models. Previous estimates of expected alpha losses from high current TFTR discharges were calculated with ripple alone or with collisions alone and were found to be about 5-10% [12–14].

Sections 2 and 3 discuss the physics of stochastic ripple diffusion and details of the ORBIT code and the simulation procedure. In Section 4, the experiments simulated are presented. In Section 5, results are compared with the experimental beta discrepancies for neutral beam ions, and with particle losses calculated by analysis codes for both neutral beam ions and alpha particles. Section 6 covers toroidal field-error-dependent stochastic diffusion losses and in Section 7 a summary and conclusion are presented.

2. Collisional Stochastic Ripple Loss Physics

2.1. *Stochastic Ripple Loss Criterion*

Goldston, White and Boozer [5] have derived a criterion for stochastic ripple loss

$$\delta_s = (\epsilon/(N\pi q))^{1.5}(1/\rho q')$$

where ϵ = aspect ratio, N = number of coils, q is the plasma safety factor, $q' = dq/dr$ and ρ is the ion Larmor radius. Trapped ions whose turning point lies in a region where δ, the toroidal field ripple, exceeds the threshold δ_s are subject to stochastic ripple diffusion. An empirical factor of 1/2 has often been included in the stochastic ripple loss criterion [11, 12], although Boivin found that the pitch angle dependence of fusion product protons on TFTR was in better agreement with the original published criterion. In Sec. 5.1 the stochastic diffusion free regions are shown for each experiment modelled. The criterion was derived in a low β, cylindrical approximation. It provides a simple, rough estimate for the stochastic ripple diffusion-free domain for specific experiments.

2.2. *Ion Pitch Angle Dependence*

Ripple and first orbit ion losses are strongly dependent on ion pitch angle. Pitch ($v_{//}/v$) describes how much of an ion's energy is in gyromotion and how much is in parallel motion along field lines. The distribution in pitch determines the trapped fraction. When a banana-trapped ion is near the bounce point (where $v_{//}$ =0), it is most strongly affected by the nonaxisymmetric tokamak magnetic field.

In Ref. [12] Boivin plotted the topology of pitch angle and turning point radius dependence for trapped, passing, first orbit lost and stochastic ripple lost 3 Mev protons for a 1.4 MA TFTR plasma. The details of the plot will change with variation in ion energy, plasma current, major radius, *etc.* but the topology will not. Fig. 1 is a cartoon based on this figure which is helpful in visualizing the different physical processes affecting the fast ions under study. In particular, pitch angle scattering causes trapped (and passing) ions to move into the stochastic ripple and first orbit loss domains.

2.3. Collision Rates

Collision frequency formulae for pitch angle scattering ($\nu_{PA} = \nu_\perp/2$) and slowing down processes are given below [28]. The definitions of the collisional scattering rates are

$$\frac{d\mathbf{v}_\alpha}{dt} = -\nu_s^{\alpha/\beta}\mathbf{v}_\alpha$$

$$\frac{d}{dt}(\mathbf{v}_\alpha - \bar{\mathbf{v}}_\alpha)_\perp^2 = \nu_\perp^{\alpha/\beta} v_\alpha^2$$

$$\frac{d}{dt}(\mathbf{v}_\alpha - \bar{\mathbf{v}}_\alpha)_\parallel^2 = \nu_\parallel^{\alpha/\beta} v_\alpha^2$$

$$\frac{d}{dt}v_\alpha^2 = -\nu_\epsilon^{\alpha/\beta} v_\alpha^2.$$

For alphas slowing down on electrons

$$\nu_s^{\alpha/e} \simeq \frac{1.6 \times 10^{-9} n_e Z^2 \lambda_{ie}}{\mu T_e^{3/2}}$$

For pitch angle scattering rates of alphas and neutral beam ions on thermal ions

$$\nu_\perp^{i/i'} = 1.8 \times 10^{-7} \frac{n_{i'} Z^2 Z_{i'}^2 \lambda_{ii'}}{\mu^{1/2} \epsilon^{3/2}}.$$

The energy slowing down rate for alpha particles is given by

$$\nu_\epsilon = 2\nu_s - \nu_\perp - \nu_{||}.$$

The energy slowing down rate for neutral beam ions is

$$\nu_\epsilon^{i/i'} = 1.8 \times 10^{-7} n_{i'} Z^2 Z'^2 \lambda_{ii'} \mu^{1/2} / \epsilon^{3/2} \mu'.$$

In our simulations, neutral beam and alpha orbits were followed with pitch angle scattering and energy slowing down effects.

3. Guiding Center Code ORBIT Simulations

To test whether ripple losses are significant on TFTR, a Monte Carlo Hamiltonian coordinate drift orbit guiding center code was used [7], with minor modifications. The code was run with plasma equilibrium flux surfaces generated by the PEST equilibrium code [29, 30]. Plasma pressure and q profiles from TRANSP simulations of specific TFTR experiments, were input to the PEST code. The equilibrium was then mapped into the Hamiltonian coordinates used by the guiding center code.

The guiding center code was used to follow 256 orbiting particles in a magnetic geometry given by

$$B = B(\Psi, \theta)(1 + \delta sin N\phi)$$

with B(Ψ, θ) from the PEST equilibrium and $\delta(\Psi, \phi)$ given by

$$\delta = \delta_o exp\{[(R_o + rcos\theta - R_{rip})^2 + b_{rip}(rsin\theta)^2]^{1/2} / w_{rip}\}.$$

Here R_o is the plasma major radius, R_{rip} =2.25 m is the major radius of the center of the ripples, b_{rip} = 1.1 is the ellipticity, δ_o is 0.000014 and w_{rip} = 0.185 m is the scale length of the ripples. There are N = 20 toroidal field coils on TFTR. Ripple, δ, on TFTR increases to about 2% at the tokamak outer midplane wall. In Fig. 2 are shown the TFTR ripple contours.

The particle distributions were generated by Monte Carlo techniques with random initial pitch and poloidal angles. The neutral beam fast ion input profiles for each experiment were obtained from total beam deposition profiles calculated by TRANSP and were due primarily to electron impact ionization. Identical beam source profiles were used for all tangency radii. Alpha particle simulations assumed a model profile, similar to that predicted by TRANSP for high power supershot DT experiments.

Although the neutral beam production process causes about 20% of the beam power to be deposited in half energy and one third energy particles, only ions with full initial energies were simulated. Particles reaching the last closed flux surface were defined as lost. Total losses were integrated over half of an energy slowing down time for neutral beam ions and over a full energy slowing down time for alpha particles. Although distinction is made in Section 2 between velocity and energy slowing down rates through subscripts s and ϵ, we will denote the energy slowing down time by τ_s. The τ_s integration time for alpha particle loss was chosen because our code comparisons are done with alpha loss fractions computed with both stochastic domain models (SNAP, MAPLOS [12]) and with first orbit and collisional calculations (TRANSP) which follow the entire slowing down process. Stochastic loss domain

codes consider all particles which satisfy the stochastic criteria to be lost immediately.

Initial and final lost particle parameters were stored in a database (out of a total of 256 ions for alpha simulations and for each beam line in neutral beam simulations). The behavior of prompt and delayed ion losses as well as individual ion orbits, were studied with this database. Simulations with collisions and ripple turned on separately were carried out to investigate the relative effectiveness of each transport process. The guiding center code includes orbit calculations for both stochastic ripple lost and ripple-trapped losses, although the ripple trapped fraction is small for TFTR.

4. TFTR Experiments Simulated

Plasma parameters for the four TFTR experiments for which fast ion orbits were followed are shown in Table I. Three of the experiments, with plasma currents of 0.9, 1.0 and 1.8 MA had major radius 2.6 m, while the fourth experiment, a high performance supershot, was carried out at 1.6 MA and major radius 2.45 m [31]. Neutral beam orbits were simulated for the R = 2.6 m cases at I_p = 0.9 and 1.0 MA. Alpha simulations were carried out for scenarios at low and high current as well as small and large major radius.

The low current experiments for which neutral beam ion orbits were simulated were designed for study of the plasma q profile, with large bootstrap current. Comparison of magnetically measured plasma beta to kinetic beta calculations in TRANSP lead to beta discrepancies of 28% for the experiment at 0.9 MA and 8% for the experiment at 1.0 MA (Table I). The two experiments were characterized by different fractions of co-going (injection

direction parallel to I_P) and counter-going ions. The neutral beam ions for the experiment at 0.9 MA were injected along six lines of sight with tangency radii given by R_T = -2.29, -1.99, -1.74 m for counter-going ions and 2.23, 1.99, 1.80 m for co-going ions. R_T is the distance of closest approach to the tokamak center. Counter-going ions are subject to signficant first orbit losses unlike co-going ions, for which the unperturbed orbits are entirely within the last closed flux surfaces. The Larmor radius for the 95.2 kev full energy deuterium ions is 1 cm, with the banana width at the plasma edge being 14.5 cm wide. Table II shows Larmor radii for fast neutral beam and alpha ions.

In Table III are shown simulation parameters for the neutral beam and alpha particle orbits studied, including pitch angle scattering collision rates and energy slowing down times. These rates were assumed constant in radius. A sensitivity study with radial variation of collision rates is discussed in Sec. 5.4.6. In the Table, T_{tran} is the toroidal transit time of a fast ion at the magnetic axis with pitch = $v_{//}/v$ = 1. ω_c is the gyrofrequency in 10^8 radians per second.

Alpha particle orbits were also simulated at I_P = 0.9 MA, R = 2.6 m, as well as for two other typical TFTR experiments. These other scenarios, similar to planned DT experiments, were a no-ICRH baseline case at I_P = 1.8 MA, R =2.6 m and a high power supershot at I_P = 1.6 MA, R = 2.45 m. Model alpha profiles were assumed and simulations were carried out for these experimental scenarios, although the original experiments were deuterium only. Simulations for the 1993-1994 TFTR DT experiments [32, 33] are in preliminary stages.

5. Results and Discussion

5.1. *Stochastic Diffusion Free Domains*

Contours in Fig. 3 bound the stochastic diffusion-free regions, for $\delta/\delta_s = 0.5, 1.0, 2.0$ criteria obtained with the Goldston, White, Boozer model. Contours are shown for fast neutral beam ions and alpha particles for experiments at 0.9 MA and 2.6 m (3a, 3b), at 1.6 MA and 2.45 m (3c, 3d), as well as for neutral beam ions, alpha particles and RF heated He^3 ions (700 keV) at 1.8 MA and 2.6 m (3e, 3f, 3g). We see that ripple is not expected to cause neutral beam losses for the R = 2.45 m case and that there is a much larger region free of stochastic ripple diffusion for alphas for this shot (Fig. 3d), compared to the low current experiment at 2.6 m (Fig. 3b), for which the model predicts a vanishingly small stochastic free region. The toroidal field ripple is smaller for plasmas with vacuum magnetic field axis at small major radius; at higher currents like 1.6 MA, the stochastic loss threshold is larger and more difficult to exceed. The threshold at R = 2.6 m, I_P = 1.8 MA (Fig. 3f) is more similar to the 2.45 m case (Fig. 3d) than to the R = 2.6 m, I_P = 0.9 MA experiment (Fig. 3b), because the variation in q_a is so much stronger than the variation in major radius in these plasmas. Figs. 3f and 3g show a reduced stochastic free region for alpha particles compared to 700 keV He^3 RF minority ions.

Figs. 3f and 3g were used to interpret recent TFTR alpha charge exchange measurements, which had detected only He^3 signals during RF, but not alphas at the half radius [34, 35]. The alpha charge exchange measurements only see trapped ions in the plasma at a location

illuminated by pellet injection. Since pellet injection has reached only to the half radius in the recent data, and pellet injection occurs after the beams are turned off, the alphas appear to have been lost by stochastic ripple diffusion, while RF ions remain in the larger stochastic ripple free region, and are observed with the diagnostic. Plans are being made for deeper pellet injection as well as for pellet injection during beam heating to study confined alpha particles. Parks [24] has developed an analytic model for the alpha distribution function expected with stochastic ripple diffusion.

5.2. *Neutral Beam Ion Diffusion*

Table IV and Figs. 4 and 5 show predicted losses of the neutral beam ions for both low current cases simulated with ripple and collisional transport. In the Tables 'Prompt' means losses occurring within twenty-five toroidal transits. For neutral beam ions this is within 150 μsec and for alpha particles this is within 35 μsec, since toroidal transit times for the two species are different (Table III). The column in Table IV labelled 'Prompt' is predominantly first orbit loss. The nonmonotonic variation of 'Prompt' losses with R_T results from the topology shown in Fig. 1. Ripple and collisions cause a loss of 23% of the fast ions during $\tau_s/2$ for the 0.9 MA experiment. First orbit losses are included in this total. TRANSP calculations (which include collisions but not ripple) predict 8% neutral beam ions lost. Figs. 4 and 5 show that the diffusion process is still nearly linear with time at $\tau_s/2$ in these simulations. We correct for the loss of ions between $\tau_s/2$ and τ_s by multiplying the loss rates by 1.5. These simulations are very expensive in computer time consumed and $\tau_s/2$

was chosen to minimize computer time costs. The correction by 1.5 for full slowing down losses is close to the ratio 1.6 found from loss fractions of simulations accumulated over τ_s and $\tau_s/2$ at -1.74 m. The extrapolation leads to 34% ion losses in τ_s. from which we subtract the TRANSP predicted first orbit and collisional losses (8%) and multiply the result by the beam fraction of β, $\beta^{nb}/\beta = 0.75$. The simulations predict ion losses which correspond to a reduction in plasma beta of 20%, close to the 28% beta discrepancy for $I_P = 0.9$ MA.

Table V shows the relative roles of ripple and collisions on the total prompt and delayed (non-first orbit) neutral beam losses for one counter-going and one co-going beamline from simulations of this experiment. The effect of collisions is not strong in increasing total losses compared to the 'Prompt' losses calculated neglecting collisions. Ripple alone is even less effective than collisions alone. Comparing to the 'no ripple. no collisions' case. when collisions and ripple are added separately and then together, we see a strong synergistic enhancement for ripple with collisions for both co-going and counter-going ions. The effect is not linear, in that the losses with collisions alone and with ripple alone cannot be simply added. In fact co-going ion losses are seen to be due entirely to the cooperative effect of ripple and collisions. As expected. there were no prompt losses for any neutral beam ions injected co-going. Prompt losses are not affected by the presence of collisions or of ripple. A measure of the synergism is S. defined as the 'ripple and collisions' delayed loss divided by the sum of the delayed losses obtained with ripple alone and with collisions alone. We estimate S = 5.4 for neutral beam ions on TFTR at 0.9 MA, with losses at -1.74 m and 1.80 m averaged.

Fig. 6 shows the neutral beam poloidal distribution function for lost ions at 0.9 MA at

each beam injection angle. The poloidal distribution becomes broader and extends toward 90 degrees as R_T becomes more negative.

For the experiment at I_P = 1.0 MA, with all co-going ions, the simulations predict 11% beam ions lost during $\tau_s/2$. As for the 0.9 MA case, we extrapolate to a 17% beam ion loss during τ_s. TRANSP predicts 3% first orbit and collisional losses and the beam ions contribute only 40% to beta for this case, so that the simulations account for a beta discrepancy of (17. - 3.)× 0.40 = 6%, close to the 8% discrepancy between measured and kinetically calculated beta.

In Fig. 7 are shown orbits for an initially passing neutral beam ion from the 0.9 MA case which is lost when ripple and collisions are included in the simulation. The figure shows the 'no ripple, no collisions' case (7a), and the corresponding cases as ripple and collisions are turned on separately (7c, 7b) and together (7d), assuming the same initial ion parameters. It is seen that collisions affect neutral beam ion orbits much more strongly than toroidal field ripple alone. In this figure each ion is followed for 120 toroidal transits. The accuracy of the Hamiltonian coordinate method is evident in the near perfect overlay of orbits for the simulation without ripple or collisions.

Our calculations were only carried out for full energy particles. To study differences in the transport of half and one third energy particles which each make up about 20% of the heating beams, simulations were done with half energy particles including increased pitch angle scattering (proportional to $1/\text{energy}^{3/2}$). It was found that particle losses decreased as energy decreased.

An additional source of fast particle losses might be due to δB from MHD activity. MHD was not present in either experiment above the level $\delta B/B = 10^{-3}$, which we have found is required for significant ion losses. We note that higher observed levels of MHD are correlated with a 38% beta discrepancy in a similar low current, large R TFTR experiment (shot 67255).

During the early beam phase of TFTR DT experiments, Chang has observed an axisymmetric beam driven mode (ABM), toroidal mode number =1, during which Darrow measured increased beam ion losses at the plasma midplane. This suggests that the "breathing" ABM mode moves the beam ions into regions of higher toroidal field ripple and that stochastic ripple transport causes the lost beam ion signal. A more quantitative analysis including experiments at higher plasma current is planned.

It is of interest to simulate the case of purely perpendicular injection for TFTR. Using the magnetic geometry of the 0.9 MA case with all beam lines injecting perpendicularly, the guiding center code simulations predict that 92% of the ions would be lost in $\tau_s/2$, about half of which are prompt lost. This implies increased loss of fast ions for low current ICRH plasmas.

The simulations indicate that most of the plasma energy missing from the low current experiments at 2.6 m was due to collisional stochastic ripple diffusion of fast beam ions not now included in the standard transport analysis. Additional anomalous fast ion diffusion processes were not required.

5.3. *Ripple Losses of Neutral Beam Ions on Other Large Tokamaks*

These results can be compared to neutral beam ripple losses reported for other large tokamaks. JET [18, 19] observed ripple loss of beam and RF ions in experiments which compared 32 and 16 toroidal field coil discharges. Maximum ripple increased from 1% to 12.5% with this change in coil number. Reduction in coil number was found to correlate with a reduction of 30% in plasma stored energy. Only 10% of the neutral beam ions were expected to be first orbit lost in the 16 coil experiment. The experiments are being analysed to evaluate whether pitch angle scattering into the loss cone is responsible for the additional 20% loss in plasma energy.

JT-60U [17] has large ripple losses because of large toroidal field ripple and because its neutral beam lines are arranged for nearly perpendicular injection so that a large fraction of the beam ions are trapped. R_T for JT-60U is 0.75 m, with major radius of 3.4 m. Tobita has carried out a study of neutral beam ion losses for JT-60U with the Orbit Following Monte Carlo (OFMC) code, similar to the ORBIT code used here. Most of JT-60U's ripple losses are from ripple trapping as $\alpha^* = \epsilon|sin\theta|/(Nq\delta)$ is large, unlike TFTR for which α^* is small everywhere. Calculations of the ripple loss fractions for JT-60U were found to be in good agreement with the experimental loss fractions, with a maximum loss fraction of 20% obtained when the ripple at the midplane was 1.7%.

Ions in TORE SUPRA [20] are also strongly affected by ripple, because of the small number of toroidal field coils, which are superconducting and must be far apart for effective cooling. In addition, the design of coils and vacuum vessel places the plasma close to the

toroidal field coils, in the region of highest ripple. Experiments at TORE SUPRA were analysed with a model which predicted that 30% of neutral beam ions were lost, being directly generated in the stochastic ripple-loss domain.

Experiments at DIII-D [36] did not find any indication of fast ion losses attributable to toroidal field ripple. DIII-D toroidal ripple is 1% at the plasma edge, half that of 2.6 m plasmas on TFTR. Such experiments, with low ripple and for diverted, low Z_{eff} plasmas, would not be expected to show collisional enhancement of neutral beam ion stochastic ripple loss.

5.4. *Alpha Particle Diffusion*

The guiding center code was also used to study the diffusion of a model alpha source profile. Magnetic flux geometries from TFTR DD experiments at 2.45 m and 2.6 m were chosen as typical candidate TFTR DT experiments. Results are shown in Tables VI–VIII, for simulations with collisional (pitch angle scattering and energy slowing down) and ripple loss processes considered separately and together. The guiding center code results are compared to TRANSP, SNAP and MAPLOS calculations in the Tables. There are differences in source profiles used, as the guiding center model profile $(1\text{-}(r/a)^2)^9$ is a fit to a typical TRANSP calculated profile for a D and T beam simulation. The fit is less accurate near the plasma edge and the typical TRANSP profile is slightly broader. MAPLOS uses the same model profile as ORBIT. Both SNAP and TRANSP calculate unique alpha profiles for each case assuming specific D and T beam configurations. The TRANSP calculations do not

include ripple but do include collisional losses which are small, as with ORBIT. Both SNAP and MAPLOS utilize the stochastic loss criterion model to compute the ripple loss fraction. SNAP Shafranov shifts the ion bounce points, first calculated in circular nonshifted geometry, while MAPLOS follows the ion in Hamiltonian drift orbit guiding center coordinates for a cylindrical geometry without Shafranov shift, but includes the ripple field only near the bounce point. Neither SNAP nor MAPLOS calculates collisional effects. Both the SNAP and MAPLOS stochastic ripple domain models reduce the threshold criterion by an empirical factor 1/2.

5.4.1. Alpha Particle Loss at 0.9 MA, R = 2.6 m

At I_P = 0.9 MA, R = 2.6 m ORBIT predicts that 34% of alphas would be lost after one energy slowing down time with 32% of the initial alpha source energy lost in this time. The 'Prompt' losses are 21%. Note our definition of 'Prompt' (Sec. 5.1). All four analysis codes predict high first orbit losses at 0.9 MA. The delayed losses are dominated strongly by ripple effects. Collisions are not important by themselves but only in concert with ripple diffusion, by collisional scattering of passing and trapped ions into the ripple loss domain. TRANSP, SNAP and MAPLOS predict similar total loss fractions at low current: 35%, 30% and 31%. MAPLOS underestimates the ripple losses because its lack of Shafranov shift places the alpha source farther from the exponentially increasing edge toroidal field ripple. This effect is largest for MAPLOS in this high q_a case.

5.4.2. *Alpha Particle Loss at 1.8 MA, R = 2.6 m*

For the case at I_P = 1.8 MA, R = 2.6 m, with reduced q_a, the ORBIT predicted alpha loss fraction (23% particles, 19% energy) remains large. This is a surprise, since the 'Prompt' losses at 1.8 MA are only 5-6% and the corresponding stochastic loss threshold map (Fig. 3f) does not imply high ripple losses. In fact, the collisionless ripple loss is only 6%. The collisional losses by themselves are again unimportant, but the combination of ripple and collisions increases the alpha energy loss level from 12% to 19%.

5.4.3. *Alpha Particle Loss at 1.6 MA, R = 2.45 m, Last Closed Flux Surface Limiter*

Here again as for neutral beam ions and the other alpha simulations, the individual roles of collisions and ripple are small. A synergistic enhancement when both processes are included causes the net loss across the plasma edge to be twice the 'Prompt' losses, if the limiter condition is set at the last closed flux surface. For R = 2.45 m we find 12% total particle losses when collisional losses are simulated. TRANSP finds 22%, with the same limiter condition The difference between the 22% TRANSP calculation and our 12% loss rate is attributed to the different source profiles used in the two cases.

5.4.4. *Alpha Particle Loss, with Vacuum Region, at 1.6 MA, R = 2.45 m*

The previous ORBIT code simulations for the R = 2.45 m experiment lack one important feature - the plasma vacuum region between the plasma edge and the tokamak wall. This vacuum region is not significant for the R = 2.6 m cases which fill the vacuum vessel, but

for the 2.45 m case if the last closed flux surface is used as the boundary for evaluating losses, first orbit losses are overestimated. A last closed flux surface limiter condition defines particles as lost if they pass the limiter; some ions will continue on orbits partly outside the plasma, and remain to heat the plasma during part of their orbits. Even with vacuum region calculations, stochastic ripple diffusion is expected to rapidly move affected banana orbits outward toward the limiter, so that stochastic ripple losses will not be greatly reduced as first orbit losses are.

Such simulations of the 2.45 m case, with the vacuum region included are 10-100 times more expensive in computer time than simulations with a limiter condition at the last closed flux surface, requiring 1-2K cray minutes each. The time required is increased because this is a three-dimensional calculation, and in the vacuum region both q and δ are larger, leading to shorter time steps and longer total computation times. A simulation of the 1.6 MA, 2.45 m case which included the vacuum region was carried out over $\tau_s/60$, 100 $\times$ the first orbit loss time. As for SNAP and TRANSP calculations, the first orbit losses were reduced to 5.5% from 9%. The ORBIT code total loss fraction was 8.6%. The total loss minus the first orbit loss for the vacuum region simulation was found to be 3% and for the last closed flux surface simulation the total loss minus the first orbit loss over this time scale was 1%. The increase in stochastic loss rate when the vacuum region is included is due to more trapped ions, available for diffusion, which are not first orbit lost. Reduced stochastic losses were not found when the vacuum region was included in the calculations. Extrapolated values in Table VIII assume that stochastic losses are unchanged when the vacuum region is included.

If the loss criterion is set to model a vacuum region rather than at the last closed flux surface, we expect that guiding center calculations will yield about 5% first orbit losses plus 12% delayed losses and 17% total alpha losses for the 2.45 m, 1.6 MA case.

5.4.5. *Collision Modelling Sensitivity Study*

Constant values for the pitch angle and slowing down rates could be improved by using radially dependent pitch angle scattering and drag rates. A sensitivity study was carried out using the radial behavior of collision rates as calculated by the TRANSP code for the R = 2.6 m, I_P = 1.8 MA experiment (Table IX). The radial variations of these rates are given by $\nu_c(r) = 1.3/(1. - (.65/.75) \times r/a)$ and $\nu_{PA}(r) = 0.1/(1. + 2.5 \times r/a)$. The radially varying rates are normalized to the constant rates (0.039 sec^{-1}, 3.3 sec^{-1}) at the half radius. Simulations were also done with constant collision rates, comparing doubled pitch angle scattering (*i.e.*, Z_{eff} increased by a factor 2), to halved pitch angle scattering (Z_{eff} reduced by a factor of 2), and to zero pitch angle scattering. Simulations with radially varying rates and with doubled scattering predicted the same loss fractions within 2% as for the baseline simulations. Reducing Z_{eff} by a factor of two reduced the overall stochastic ripple diffusion losses by only about one-third. The saturation in particle losses as Z_{eff} increases occurs because only particles near the boundary of the loss regions can be collisionally driven into the loss cone during a slowing down time.

5.4.6. *Summary Discussion of Alpha Losses*

Fig. 8 shows individual alpha orbits for an initially trapped alpha particle, which is lost from from the $I_P = 0.9$ MA, R = 2.6 m case when both ripple and collisional processes affect the orbit. The figure shows the no ripple, no collision case as well as orbits which result from adding collisions and ripple separately and together. These simulations all assume the same initial alpha parameters and follow the ion for 120 toroidal transits.

Ripple is seen to affect the alpha particle orbit more strongly than collisions. This different effect, in comparison with neutral beam ions (Fig. 7), can be understood as follows. Because the diffusion coefficient for stochastic ripple transport is that of ripple plateau, D $=\Delta^2\omega_b$, stochastic ripple diffusion is 150 times larger for alphas than for neutral beam ions. Since pitch angle scattering rates are inversely proportional to energy, the neutral beam ion pitch angle scattering rate is 100 times that of alphas in the same experiment (Table III), and the orbits of the less energetic neutral beam ions are more strongly affected by pitch angle scattering than are orbits of alpha particles.

Increased pitch angle scattering into the first orbit loss cone at low energies might have been expected to increase particle losses significantly. But, since adding collisions to the 'no ripple, no collisions' cases does not increase ion losses by more than a few percent, the reduction of the ion banana width by slowing down must nearly cancel the effect of the increased pitch angle scattering at low energies.

In Fig. 9 are shown the total losses calculated as a function of time for the three TFTR cases studied. Note the suppressed zeroes; the prompt loss fractions are different for each

case. The diffusive nature of the process is evident from the figure, with longer diffusion times for low current and for large major radius. The relative rates of pitch angle scattering to slowing down for alphas are similar in all three cases ($\nu_{PA}/\nu_\epsilon = 0.007, 0.012, 0.011$). The faster evolution for the 2.45 m plasma results from lower toroidal field ripple at small major radius and a smaller stochastic ripple domain (Fig. 1).

Figs. 10-12 show the initial ion parameters for alphas lost from the guiding center code simulations of the three projected DT TFTR experiments. The ion lifetimes are indicated by symbol with white diamonds and squares for first orbit loss events. The first orbit loss and the stochastic ripple loss region topologies are similar to Fig. 1. The first orbit loss region is much narrower for 1.8 and 1.6 MA (Figs. 11-12). Delayed loss events due to diffusion of passing particles into the prompt orbit loss cone from below as μ increases due to pitch angle scattering appear when collisions are added to the no ripple, no collisions case. In all three cases these events occur only after alpha lifetimes greater than 2000 μsec (black squares). Delayed loss events representing diffusion of trapped particles from above into the ripple domain (due to reduction of μ by pitch angle scattering) and events due to collisionless stochastic ripple loss, are denoted by black diamonds and squares, for alpha lifetimes between 50 and 2000 μsec and greater than 2000 μsec. Most 'Prompt' losses are within the 10 microsecond time scale thought to characterize first orbit losses in fusion product measurements [12–14]. A statistically significant population characterized by time scales of 50-2000 μsec arises when ripple is added to the collisional simulations of the 0.9 MA case.

Fig. 13 is a summary figure which combines results from high and low current ORBIT simulations at 2.6 m. The I_P dependence of first orbit losses, collisional losses, stochastic ripple diffusion (collisionless), and collisional stochastic ripple diffusion, as well as the total losses are shown. Collisional losses are small; first orbit losses decrease rapidly with increasing plasma current; stochastic ripple losses are < 10% but collisional stochastic ripple losses are 10 – 20% and do not decrease as plasma current increases. They increase with plasma current for these simulations because the ratio of pitch angle scattering to slowing down increases with plasma current (ν_{PA}/ν_ϵ = .007 at 0.9 MA, ν_{PA}/ν_ϵ = .012 at 1.8 MA, Table III). The higher current experiment with high T_e had a longer alpha slowing down time. This caused increased collisional stochastic ripple diffusion for the higher I_P experiment. In general, higher plasma heating power can be used at increased plasma current, leading to higher electron temperatures so that increased CSRD is expected at high I_P. The synergistic enhancements are S = 1.4, 2.4, 1.5 for the alpha loss fractions of Tables VI-VIII.

5.4.7. Comparison with Experiment

Initial analyses of 1993-1994 TFTR DT experiments by Janos [37] for wall heating and by Darrow [38] for alpha loss do not require alpha loss rates greater than 20-30%, as predicted by these simulations.

Zweben [39] has observed a delayed loss of DD fusion products at 90 degrees below the plasma midplane in R = 2.45 m plasmas, but not in 2.62 m plasmas. It is interesting to see what our simulations predict for the poloidal and pitch angle distributions of fast particle

losses. Figs. 14 and 15 show the predicted poloidal and final pitch angle distributions of 'Prompt' and total loss fractions for alpha particles as calculated for the TFTR experiments at 0.9 MA and 1.8 MA. The figures show the fractions lost as a function of poloidal angle in units of radians and as a function of the cosine of the pitch angle.

Fig. 14 shows losses peaked just below the midplane in all cases with the prompt loss events being much less strongly peaked about the midplane than the total of prompt and stochastic losses. The low current case shows a greater likelihood of events at 90 degrees than the 1.8 MA case. Some alpha loss events are predicted near the 90 degree detector location, while simulations of neutral beam ions (Fig. 6) lead to no events at 90 degrees for either current. ORBIT's ratios of alpha loss events at 20±5 degrees to those seen at 45±5 degrees are as follows: $R_{loss} = 4/3$ for 0.9 MA and $R_{loss} = 11/2$ at 1.8 MA, while less variation (3/2) is seen in comparing 0.9 MA to 1.8 MA at 45 degrees. With a window of ±10 degrees at 45 degrees the ratio of lost alphas at 0.9 MA to those at 1.8 MA is 3/6, reflecting the increased stochastic loss rate at high current.

What do these time dependent results suggest concerning the delayed losses observed by Zweben [39] at 2.45 m but not at 2.62 m? The long time scale is compatible with the simulations of *collisional* stochastic ripple diffusion. Although most stochastic losses do take place quickly after the birth of the particle, there will always be some losses later in the ion's lifetime, as the eventual effect of pitch angle scattering plus ripple deformation of field lines and ion orbits accummulates (Fig. 9). More fusion products from plasmas at 2.62 m are born in regions of strong ripple than at 2.45 m and a greater fraction are quickly lost through

collisionless stochastic ripple diffusion. At 2.45 m, more fusion products not immediately lost to stochastic ripple diffusion are available to be collisionally driven into the stochastic loss region and the first orbit loss cone during the ions' slowing down time.

5.5. *Control of Stochastic Ripple Loss*

How can these collisional stochastic ripple losses be controlled in a tokamak with nonzero edge ripple? The simulation results showed that the diffusive effect of stochastic ripple losses on fast ions is greatly enhanced by the presence of collisions. The resulting losses can be reduced by shortening the energy slowing time so that pitch angle scattering losses do not accumulate, by reducing the pitch angle scattering rate or by increasing the size of the stochastic free region by reducing the ripple strength. The formulae for collision rates were given in Sec. 2.3. Since

$$Z' \sim \mu'/2$$

we see

$$\nu_c^{i/i'} \sim n_{i'} Z' \sim n_e,$$

and

$$\tau_c^{i/i'} \sim 1/n_e.$$

We note also that

$$\nu_c^{\alpha/e} \sim n_e T_e^{-3/2}$$

so that

$$\tau_c^{\alpha/e} \sim T_e^{3/2}/n_e$$

and that

$$\nu_{\perp}^{i/i'} \sim n_{i'} Z_{i'}^2 \sim n_e Z_{eff}.$$

Pitch angle scattering can be reduced for both neutral beam and alpha particles in plasmas if Z_{eff} is lowered. Operating at lower T_e, as in pellet experiments, will shorten $\tau_\epsilon^{\alpha/e}$. $\tau_\epsilon^{\alpha/e}$ and $\tau_\epsilon^{i/i'}$ will be reduced for experiments at higher n_e. But since $\nu_\perp$ is also proportional to n_e, control of ripple losses would require tuning the density to find the optimal value for reduced pitch angle scattering and shortened slowing down time.

A method for burn control for fusion reactor operation may be achievable through this collisional control of stochastic ripple diffusion. Impurity puffing or injection at the plasma edge could be applied to vary Z_{eff}, T_e, *etc.* during reactor operation. Care would be needed not to trigger quenching of ignition or disruption, and to prevent excessive localized wall heating. Fisch [40] has recently suggested that RF could be used to rapidly catalyze direct conversion of alpha particle energy into the energy of D and T reactor fuel ions. If the catalysis is rapid and efficient enough (within 25–50 μsec) non-first orbit alpha particle energy can be utilized for fusion before stochastic ripple losses occur.

6. Toroidal Field Error Induced Fast Ion Losses

Owens and Janos have measured the actual vacuum TFTR field and have produced a model for field errors due to radial displacements of -1.0, -2.0, -2.0, 1.8, 1.8 cm for TFTR coils 2–6 (Fig. 16). (They also found a rotation of .04 degrees for the fourth coil.) This is about the same size as the toroidal field ripple at the plasma center. At R = 2.95 m, the

toroidal field ripple is 0.0006, and the toroidal field error is 0.0005. With an effective coil number of 3, rather than 20, δ_s is increased by a factor of 17. Consequently the stochastic criterion is not likely to be exceeded by the field error, in the outer half of the plasma where ripple is dominated by the discreteness of the coils. Toroidal field errors are not expected to cause significant fast ion losses for most planned experiments at TFTR.

Johnson and Reiman [41] have looked into the effect of plasma currents interacting with the plasma ripple at finite beta and find that the dominant effect comes from the Shafranov shift of the magnetic axis so that a greater fraction of the plasma is in the ripple domain. This effect has been included in our work. Other intrinsic plasma response to the ripple field is not expected to be large.

7. Conclusion

Monte Carlo Hamiltonian coordinate following code simulations of two low current TFTR experiments predict that 23% and 11% of the injected neutral beam ions were lost due to 'Prompt' and collisional stochastic ripple diffusion over $\tau_s/2$ and thus resolve kinetic transport analysis discrepancies of 28% and 8% with measured beta. Additional anomalous fast ion transport was not found necessary for neutral beam ions. The poor performance of large major radius, high q_a supershots appears to be due to these prompt and collisional stochastic ripple losses.

A synergistic enhancement for ripple with collisions was found to increase the total losses for neutral beam ions and alpha particles. 20% losses of alpha particles and alpha heating

are projected for DT experiments on TFTR at 2.6 m for 1.8 MA plasmas, with higher losses at lower current. Toroidal field error induced fast ion losses, due to imperfectly aligned coils, are expected to be small on TFTR.

The guiding center code simulations showed enhanced fast ion losses with ripple and collisions acting synergistically. Consideration of scattering rates suggests that operating at low Z_{eff} will keep ripple diffusion losses low by reducing pitch angle scattering and that alpha loss can be minimized by operating at lower T_e to shorten slowing down times. Alpha losses will be minimized if I_p is large and R is small, as for most planned TFTR DT experiments. However, discharges at large R to study RF heating and current drive and discharges at low current, will be subject to stronger ripple diffusion so that control of these losses by operating at reduced Z_{eff}, T_e, *etc.* is even more desirable. Experimentally validated computer simulations of fast ion collisional stochastic ripple diffusion are needed for the design of future fusion devices like TPX [42], SSTR [43], and ITER [44], for which ripple losses of alphas are now a central issue.

Acknowledgment

The authors would like to acknowledge many useful discussions with R. Boivin, C. S. Chang, Z. Chang, D. Darrow, E. Fredrickson, A. Janos, S. Medley and K. Owens. Assistance by M. Manickam with the PEST code and by M. Chance with the MAPPING code is gratefully acknowledged. We thank K. Owens and A. Janos for supplying Fig. 16. PPPL research students A. Smitten and A. Marks contributed excellent computational support.

We are glad to thank R. Goldston, R. Hawryluk and K. McGuire for their interest in this problem. This work was supported by the U. S. Department of Energy Contract No. DE-AC02-76-CHO-3073.

References

[1] P. N. Yushmanov, Nuclear Fusion **23** (1983) 1599.

[2] P. N. Yushmanov, J. R. Cary, S. G. Shasharina, Nuclear Fusion **33** (1993) 1293.

[3] C. S. Chang, S. J. Zweben "An Approximate Analytic Model for Collisional Loss of Energetic Ions into a Tokamak First Orbit Loss Cone" PPPL - (1994), submitted to Nuclear Fusion.

[4] A. H. Boozer, Phys. Fluids **23** (1980) 2283.

[5] R. J. Goldston, R. B. White, A. H. Boozer, Phys. Rev. Lett. **47** (1981) 647.

[6] S. G. Shasharina, J. R. Cary, Nuclear Fusion **33** (1993) 648.

[7] R. B. White, M. S. Chance, Phys Fluids **27** (1984) 2455.

[8] R. B. White, Phys. Fluids **B2** (1990) 845.

[9] R. B. White, Theory of Tokamak Plasmas, North Holland Pub. Co., 1989, Amsterdam, 361 pp.

[10] R. J. Goldston, H. H. Towner, J. Plasma Physics **26** (1981) 283.

[11] S. D. Scott *et al.*, Nuclear Fusion **25** (1985) 359.

[12] R. L. Boivin, S. J. Zweben, R. B. White, Nuclear Fusion **33** (1993) 449.

[13] S. J. Zweben, *et al.* IAEA conference, **1** (1992) 363, Wurzburg, Germany.

[14] R. V. Budny, "A Standard DT Supershot Simulation", Nuclear Fusion (1994) in press.

[15] R. B. White, H. E. Mynick, Phys. Fluids **B1** (1989) 980.

[16] S. J. Zweben, R. L. Boivin *et al.*, Nuclear Fusion **31** (1991) 2219. Sept (1993) 61pp.

[17] K. Tobita, K. Tani, *et al.*, Phys. Rev. Lett. **69** (1992) 3060–3063.

[18] G. Sadler *et al.*, in *Proceedings of the 1992 International Conference on Plasma Physics, Innsbruck* (European Physical Society, Petit-Lancy, Switzerland, 1992), Vol. 1, p. 167;

[19] B. Tubbing, *et al.* 14th IAEA Conf. On Plasma Physics and Controlled Fusion Research, Wurzburg, 1992.

[20] V. Basiuk *et al.*, in *Proceedings of the 1992 International Conference on Plasma Physics, Innsbruck* (European Physical Society, Petit-Lancy, Switzerland, 1992), Vol. 1, p. 175.

[21] K. Tani, T. Takizuka, M. Azumi Nuclear Fusion **33** (1993) 903-914.

[22] K. Tani, M. Azumi, *et al.*, J. Phys. Soc. Japan **50** (1981) 1726-1737.

[23] K. Tani, T. Takizuka, M. Azumi, H. Kishimoto, Nuclear Fusion **23** (1983) 657-665.

[24] P. B. Parks, R. F. Fisher, J. M. McChesney, "Effect of Stochastic Ripple Diffusion on the Detection of Fusion Product Ions by Charge Exchange Pellet Diagnostics", GA-A21689 (1994), submitted to Nuclear Fusion.

[25] H. Towner *et al.*, RSI **6** (1992) 4753.

[26] R. Hawryluk *et al.*, Proceedings of the Course on Physics of Plasmas Close to Thermonuclear Conditions (Commission of the European Communities, Brussels, 1980) Report EUR FU, BRU/XII/476/80 Vol. 1, p 19 ; R. J. Goldston *et al.*, J. Comput. Phys. **43** 61 (1981).

[27] C. W. Barnes, *et al.*, "Triton Burnup Measurements and Calculations on TFTR", in preparation; P. Batistioni and C. W. Barnes, Plasma Physics and Controlled Fusion **33** (1991) 1735.

[28] David L. Book, NRL Plasma Formulary, Washington, D. C., NRL Publication 177-4405, (1990) 64pp.

[29] R. C. Grimm, J. Greene, J. L. Johnson, Meth. Computing Physics **9** (1974) 253.

[30] R. C. Grimm, R. L. Dewar, J. Manickam, J. Comput. Phys. **49** (1983) 94-117.

[31] R. V. Budny, *et al.*, Nuclear Fusion **32** (1992) 429-447.

[32] R. Hawryluk, *et al.* "Confinement and Heating of a Deuterium- Tritium Plasma on the Tokamak Fusion Test Reactor", Phys. Rev Letters, in press.

[33] J. D. Strachan, *et al.*, "Fusion Power Production from TFTR Plasmas Fueled with Deuterium and Tritium", Phys. Rev. Letters, in press.

[34] J. M. McChesney, *et al.* Proceedings of 10th High Temperature Plasma Diagnostics Meeting, Conference, Rochester, N. Y. May 1994.

[35] S. S. Medley, *et al.*, Proceedings of the Twentieth European Physical Society Conference on Controlled Fusion and Plasma Physics (Lisbon, Portugal, July 1993) Vol. III 1183-1186.

[36] H. H. Duong, W. W. Heidbrink, Nuclear Fusion **33** (1993) 211-224.

[37] A. Janos, *et al.* Proceedings of 10th High Temperature Plasma Diagnostics Meeting, Conference, Rochester, N. Y. May 1994.

[38] D. Darrow, *et al.* Proceedings of 10th High Temperature Plasma Diagnostics Meeting, Conference, Rochester, N. Y. May 1994.

[39] S. J. Zweben, D. S. Darrow, E. D. Fredrickson, H. E. Mynick Nuclear Fusion **33** (1993) 705-724.

[40] N. Fisch, J-M. Rax, Phys. Rev. Lett. **69** (1992) 612;. N. Fisch, *et al.*, Plasma Phys. and Contr. Fusion (IAEA 92) (1993) 769; N. Fisch, Phys. Fluids **B** 5, (1993) 1754.

[41] J. L. Johnson, A. H. Reiman, Nuclear Fusion **28** (1988) 1116–1120.

[42] J. A. Schmidt *et al.*, Journal of Fusion Energy, **12** (1993) 455.

[43] M. Kikuchi, Nuclear Fusion **30** (1990) 265-276.

[44] Y. Shimomura, *et al.*, Overview of the International Thermonuclear Experimental Reactor, Physics of Plasmas, 1 (1994) 1610-1616.

Table I. TFTR Experiments Simulated

Shot	R (m)	B_T (T)	I_p (MA)	q_a	P_{inj} (MW)	$\Delta\beta$ (%)
67241	2.6	4.5	0.9	14.	13.	28.
67243	2.6	4.5	1.0	11.	9.	8.
67885	2.6	4.8	1.8	6.	23.	–
55851	2.45	5.1	1.6	5.6	25.	–

Table II. Larmor Radii for Fast Ions

Particle	Energy (kev)	Mass m_H	Charge q_e	Larmor radius (m)
deuteron	95.2	2	1	0.01
alpha	3500.	4	2	0.06

Table III. Simulation Parameters

	67241	67243	67885	55851
$\nu_{pa}^{d}(sec^{-1})$	2.5	.77	–	–
$\nu_{pa}^{\alpha}(sec^{-1})$	.030	–	.039	.047
$\tau_{s}^{d}(sec)$	.34	.73	–	–
$\tau_{s}^{\alpha}(sec)$	.23	–	.30	.23
$n_{eo}(10^{13}/cm^{3})$	3.8	2.	5.2	8.5
$T_{eo}(keV)$	6.0	6.5	9.0	10.5
$< n_{e} > (10^{13}/cm^{3})$	2.	1.	2.5	3.5
$< T_{e} > (keV)$	3.5	3.5	2.5	6.0
Z_{eff}	3.2	2.	3.3	2.9
$T_{tran}^{d}(\mu s)$	6.1	5.9	–	–
$T_{tran}^{\alpha}(\mu s)$	1.4	–	1.4	1.3
$\omega_{c}^{d}(10^{8}/s)$	2.1	2.1	–	–
$\omega_{c}^{\alpha}(10^{8}/s)$	2.1	–	2.3	2.4

Table IV. Fraction of Neutral Beam Ions Lost in Simulations of TFTR High q_a Experiments during $\tau_s/2$

R_T	Fraction Lost		
	Prompt	Delayed	Total
shot 67241	I_P = 0.9 MA		
-2.23 m	.06	.23	.29
-1.99	.14	.20	.34
-1.74	.10	.28	.38
1.80	.0	.15	.15
1.99	.0	.12	.12
2.29	0.	.07	.07
average	.05	.18	.23
shot 67243	I_P = 1.0 MA		
1.80	0.	.15	.15
1.99	0.	.10	.10
2.05	0.	.08	.08
2.29	0.	.07	.07
average	0.	.11	.11

Table V. Effect of Ripple and Collisions on Prompt

and Delayed Neutral Beam Losses

for I_P = 0.9 MA, R = 2.6 m during $\tau_s/2$

Col	Rip	R_T	Prompt	Delayed	Total
–	–	-1.74 m	.10	.00	.10
√	–	-1.74	.10	.06	.16
–	√	-1.74	.10	.02	.12
√	√	-1.74	.10	.28	.38
–	–	1.80	.00	.00	.00
√	–	1.80	.00	.00	.00
–	√	1.80	.00	.00	.00
√	√	1.80	.00	.15	.15

Table VI. Alpha Losses during τ_s for I_P =0.9 MA, R = 2.6 m (%)

Collisions	Ripple	Prompt	Delayed	Total	Energy
ORBIT:					
–	–	21.	0.	21.	21.
√	–	21.	2.	23.	23.
–	√	22.	7.	29.	29.
√	√	21.	13.	34.	32.
TRANSP:					
√	–	32.	2.	35.	
SNAP:					
–	√	23.	7.	30.	
MAPLOS:					
–	√	30.	1.	31.	

Table VII. Alpha Losses during τ_2 for I_P = 1.8 MA, R = 2.6 m (%)

Collisions	Ripple	Prompt	Delayed	Total	Energy
ORBIT:					
–	–	5.	1.	6.	6.
√	–	5.	1.	6.	6.
–	√	6.	6.	12.	12.
√	√	6.	17.	23.	19.
TRANSP:					
√	–	10	0.5	10.5	
SNAP:					
–	√	8.	9.	17.	
MAPLOS:					
–	√	5	2	7	

Table VIII. Alpha Losses during τ_s for I_P = 1.6 MA, R = 2.45 m (%)

Collisions	Ripple	Prompt	Delayed	Total	Energy
Last Closed Flux Surface Limiter					
ORBIT:					
–	–	9.	0.	9.	9.
√	–	9.	3.	12.	11.
–	√	9.	5.	14.	14.
√	√	9.	12.	21.	20.
TRANSP:					
√	–	19.	3.	22.	
SNAP:					
–	√	10.	4.	14.	
Experimental Limiter Location:					
ORBIT:					
√	√	5.5	12.[a]	17.5[a]	16.5[a]
TRANSP:					
√	–	10.	1.	11.	
SNAP:					
–	√	5.	6.	11.	
MAPLOS:					
–	√	3.	2.	5.	

[a]Extrapolation

Table IX. Alpha Losses during τ_s for I_P = 1.8 MA, R = 2.6 m with Variations in Collision Modelling

ν_{PA} (sec^{-1})	ν_s (sec^{-1})	Prompt (%)	Delayed (%)	Total (%)
.039	3.3	6.	17.	23.
$\nu_{PA}(r)$	$\nu_\epsilon(r)$	6.	16.	22.
.078	3.3	6.	19.	25.
.020	3.3	6.	11.	17.
0.	0.	6.	7.	13.

Figures

Fig. 1. The topology of trapped and passing ions and the first orbit and stochastic ripple loss domains plotted as a function of initial magnetic moment and outer midplane crossing point.

Fig. 2. TFTR ripple contours.

Fig. 3. TFTR stochastic ripple loss thresholds δ/δ_s for fast beam ions and alpha particles for 0.9 MA at R = 2.6 m (a, b); and for 1.6 MA at R = 2.45 m (c, d); for fast beam ions, alpha particles and RF heated He^3 ions at 1.8 MA and R = 2.6 m (e, f, g).

Fig. 4. Evolution of loss fractions for neutral beam ions over $\tau_s/2$ for 0.9 MA, R = 2.6 m with R_T = a) -2.23 m, b) -1.99 m, c) -1.74 m, d) 1.80 m, e) 1.99 m and f) 2.29 m.

Fig. 5. Evolution of loss fractions for neutral beam ions over $\tau_s/2$ for 1.0 MA, R = 2.6 m with R_T = a) 1.80 m, b) 1.99 m, c) 2.05 m, and d) 2.29 m.

Fig. 6. Poloidal distributions of neutral beam ions lost over $\tau_s/2$ at 0.9 MA, 2.6 m for R_T = a) -2.23 m, b) -1.99 m, c) -1.74 m, d) 1.80 m, e) 1.99 m and f) 2.29 m for poloidal angle in units of radians.

Fig. 7. Individual neutral beam ion orbits for the 0.9 MA experiment with a) ripple and collisions off; b) ripple off, collisions on; c) ripple on, collisions off; d) ripple and collisions on.

Fig. 8. Individual alpha particle orbits for the 0.9 MA experiment with a) ripple and collisions off; b) ripple off, collisions on; c) ripple on, collisions off; d) ripple and collisions on.

Fig. 9. Evolution of total loss fractions of alphas from simulations of TFTR experiments at a) R = 2.6 m, I_P = 0.9 MA; b) R = 2.6 m, I_P = 1.8 MA; and c) R = 2.45 m, I_P = 1.6 MA.

Fig. 10. Initial magnetic moments and plasma radii of lost alphas for I_P =0.9 MA, R =2.6 m with ripple and collisions as a function of ion's lifetime.

Fig. 11. Initial magnetic moments and plasma radii of lost alphas for I_P =1.8 MA, R =2.6 m with ripple and collisions as a function of ion's lifetime.

Fig. 12. Initial magnetic moments and plasma radii of lost alphas for I_P =1.6 MA, R =2.45 m with ripple and collisions as a function of ion's lifetime.

Fig. 13. Alpha loss fractions at 2.6 m, from first orbit (FO), collisional (COL), stochastic ripple diffusion (SRD), collisional stochastic ripple diffusion (CSRD) and total loss fractions (Total).

Fig. 14. Poloidal distributions of alpha particles: 'Prompt' loss events from simulations of a) the 0.9 MA experiment and b) the 1.8 MA experiment; total loss events from c) the 0.9 MA experiment and d) the 1.8 MA experiment. Poloidal angle in units of radians.

Fig. 15. Pitch angle distributions of alpha particles: 'Prompt' loss events from simulations of a) the 0.9 MA experiment and b) the 1.8 MA experiment; total loss events from c) the

0.9 MA experiment and d) the 1.8 MA experiment.

Fig. 16. Toroidal field error at R = 2.95 m on TFTR.

PPPL#94X0142

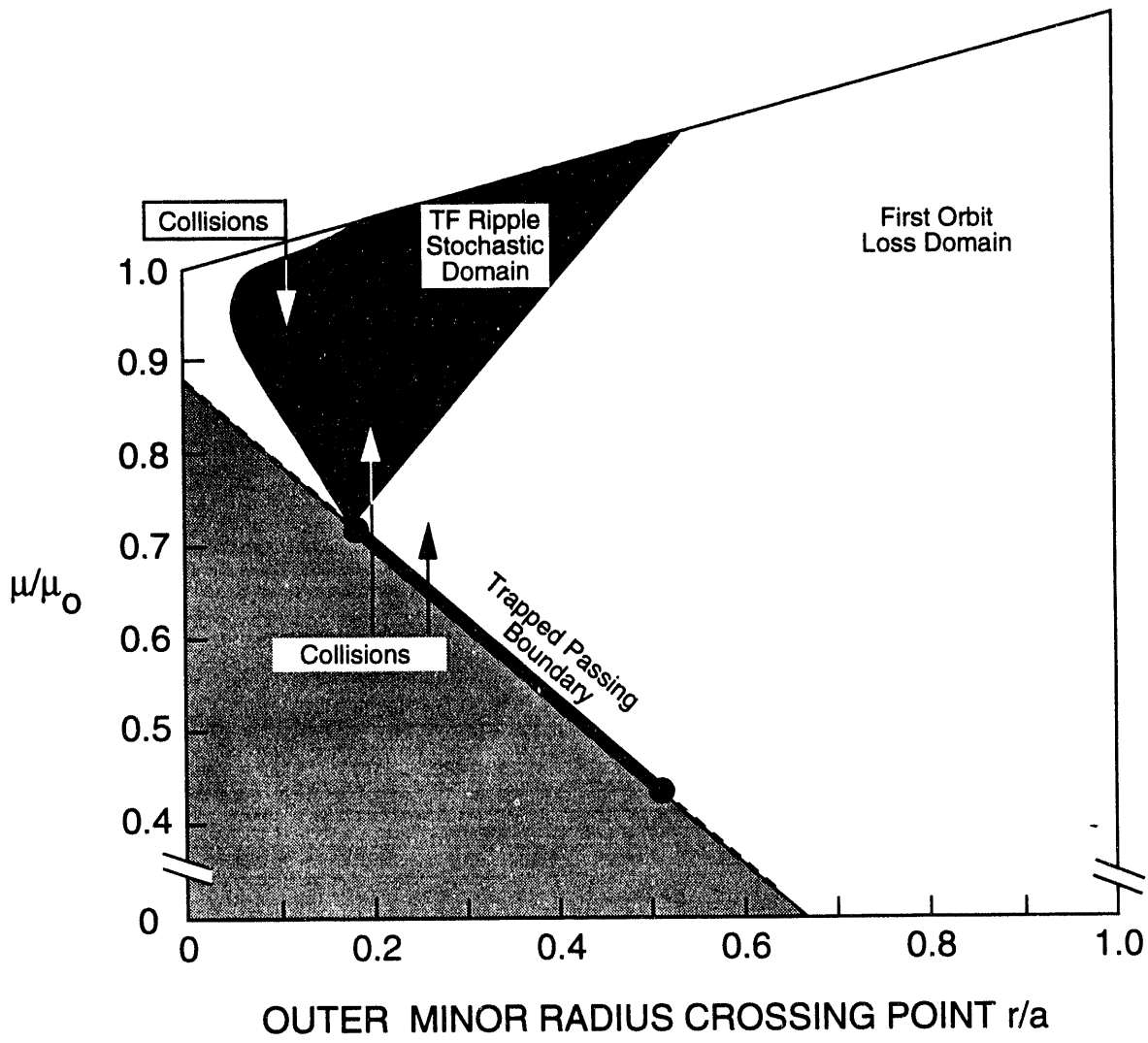

Fig. 1

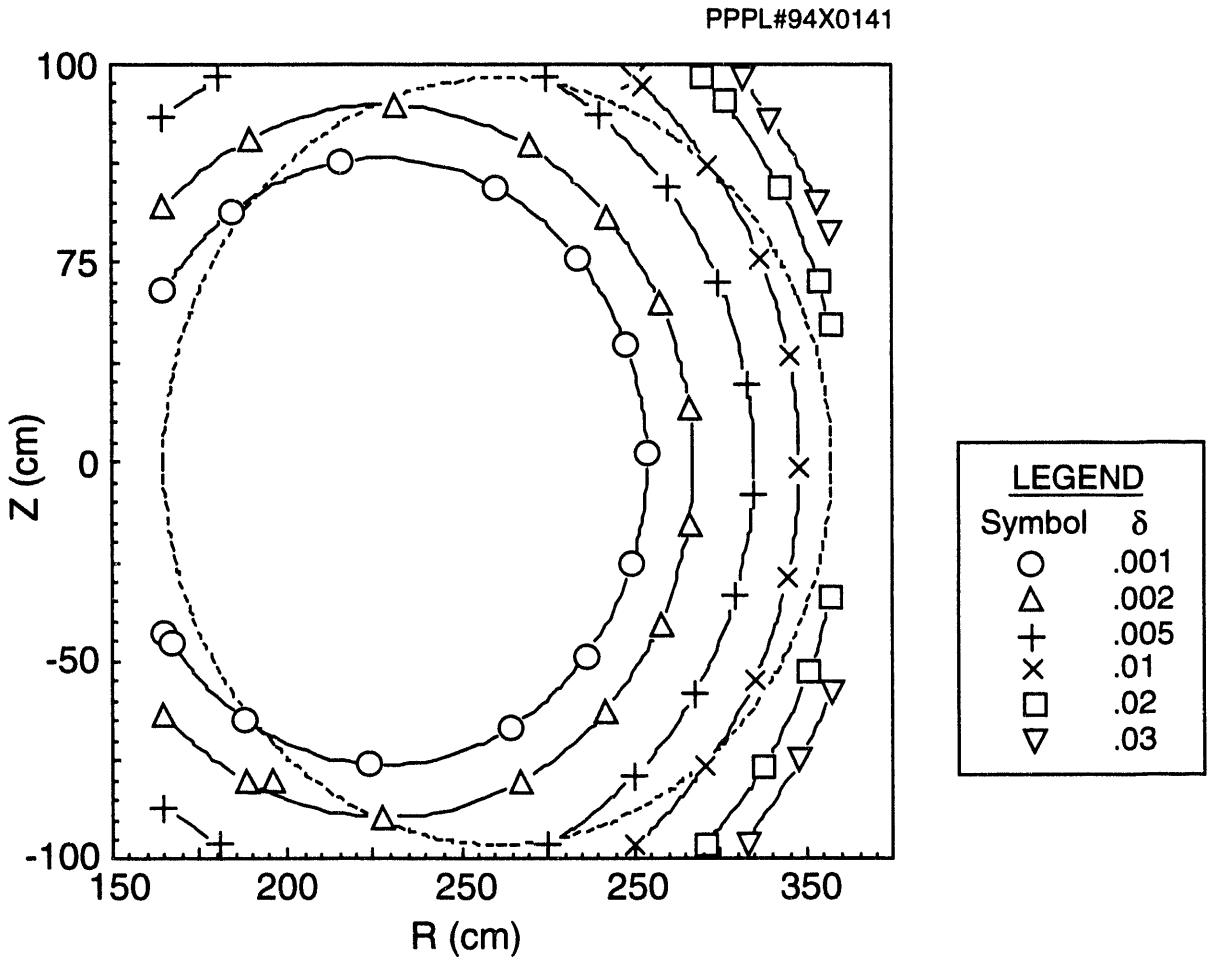
PPPL#94X0141
100
75
0
-50
-100
Z (cm)
150
200
250
250
350
R (cm)
LEGEND
Symbol δ
.001
.002
.005
.01
.02
.03

Fig. 2

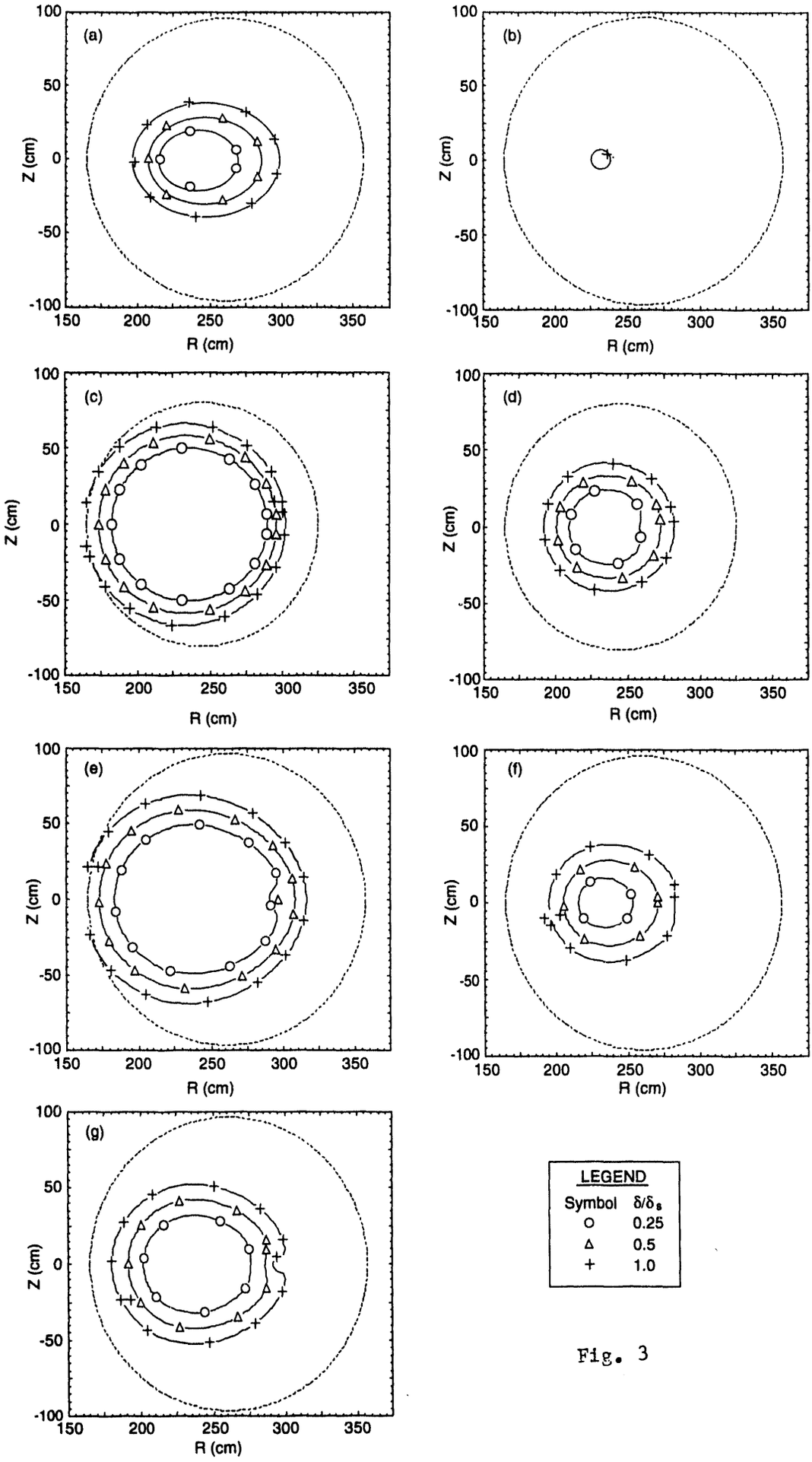
(a)
(b)
(c)
(d)
(e)
(f)
(g)
Z (cm)
R (cm)
100
50
0
-50
-100
150
200
250
300
350
LEGEND
Symbol δ/δs
○ 0.25
△ 0.5
+ 1.0

Fig. 3

PPPL#94X0143

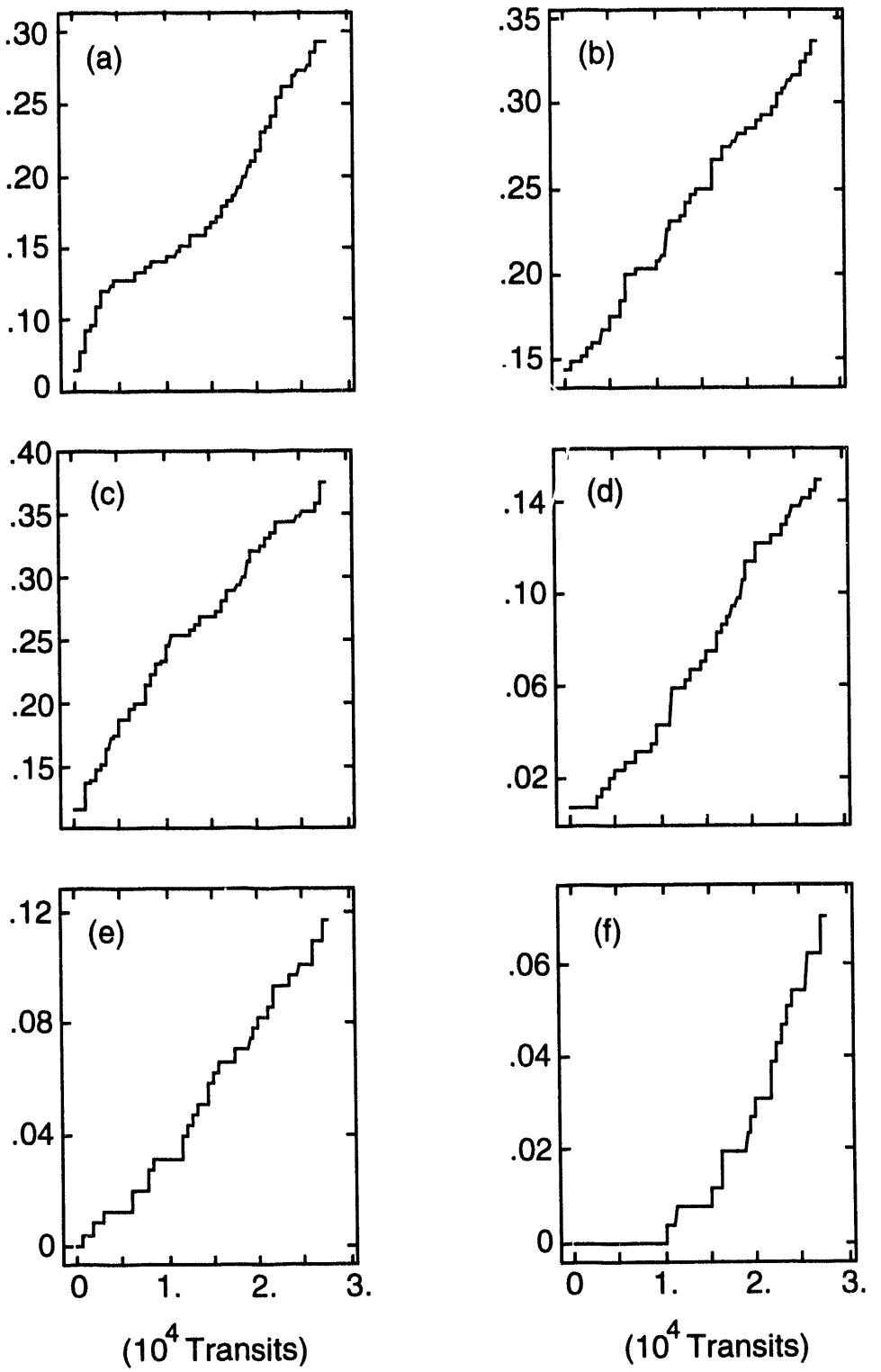

Fig. 4

PPPL#94X0144

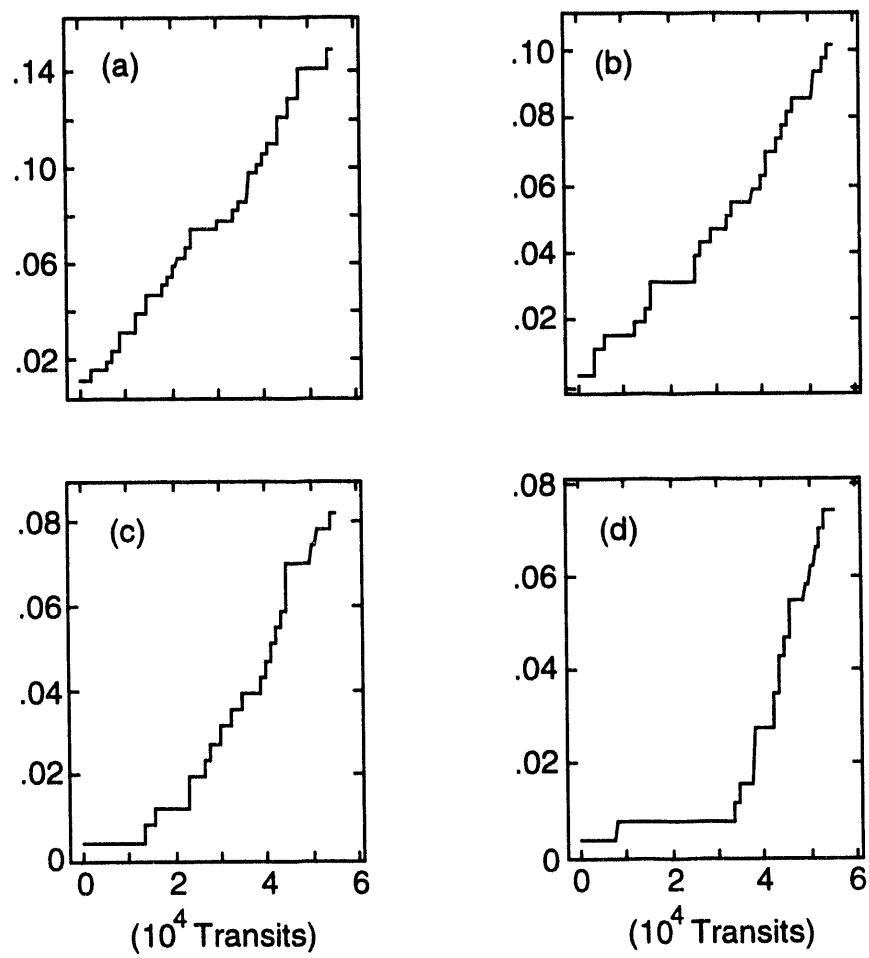

Fig. 5

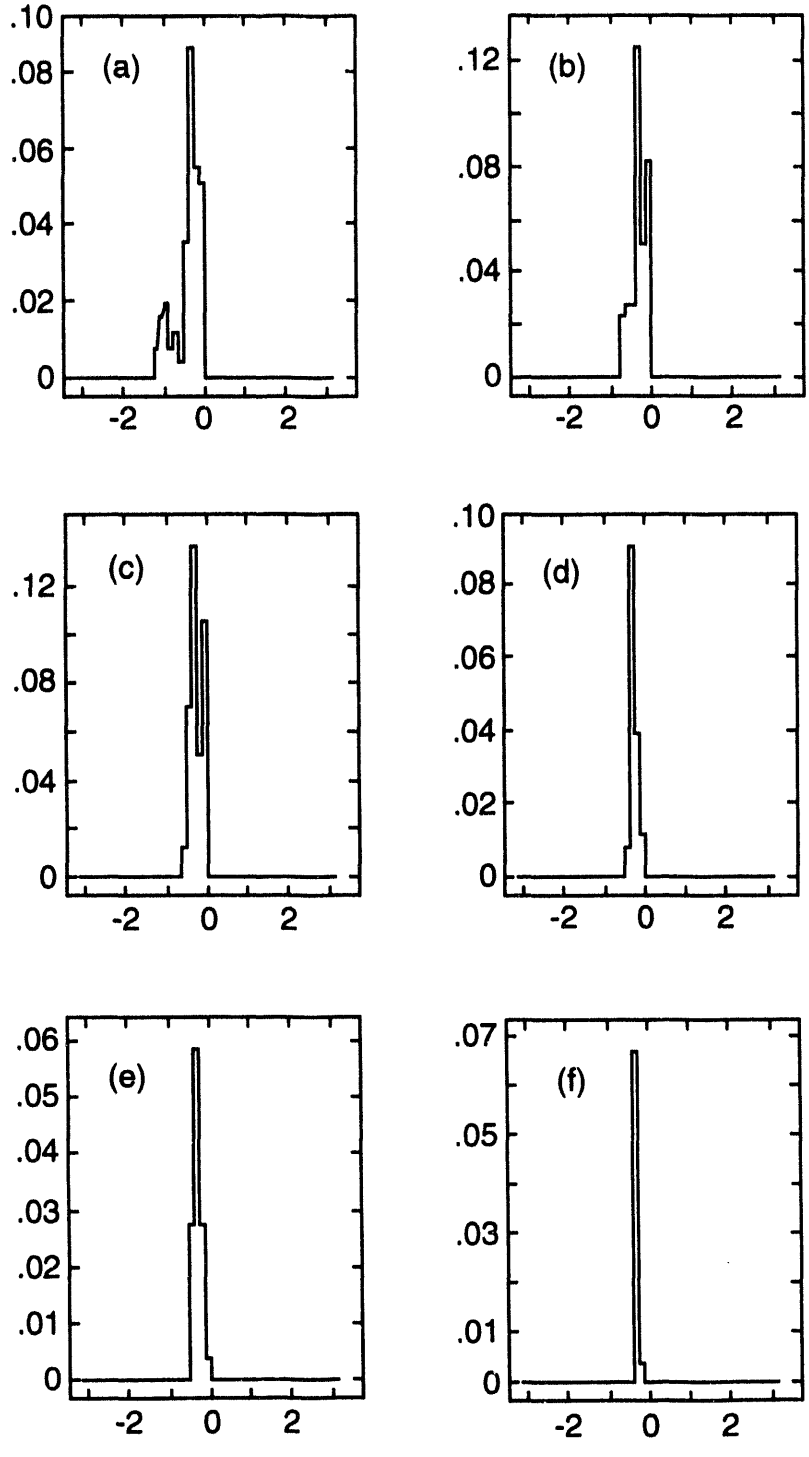

Fig. 6

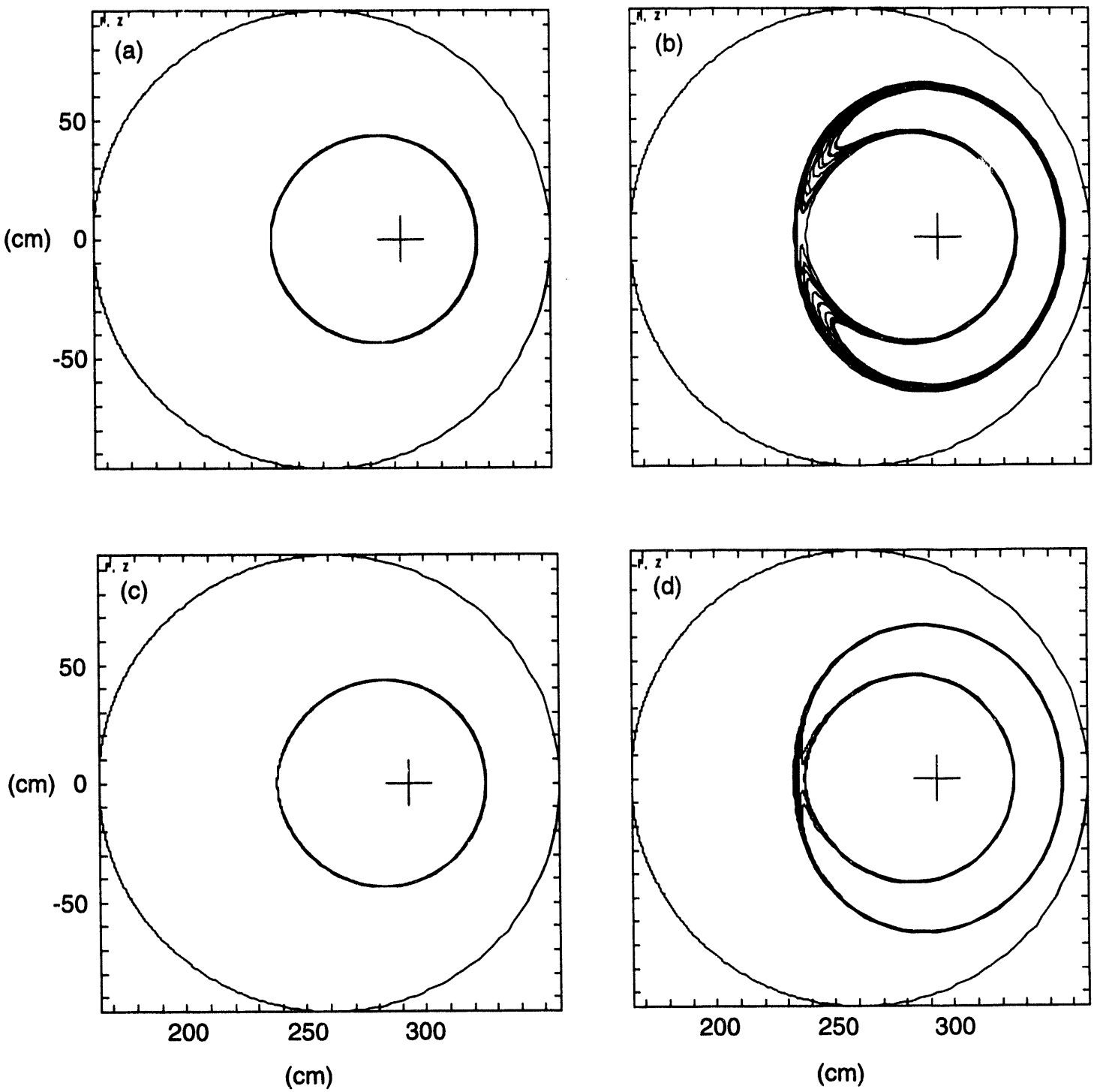

Fig. 7

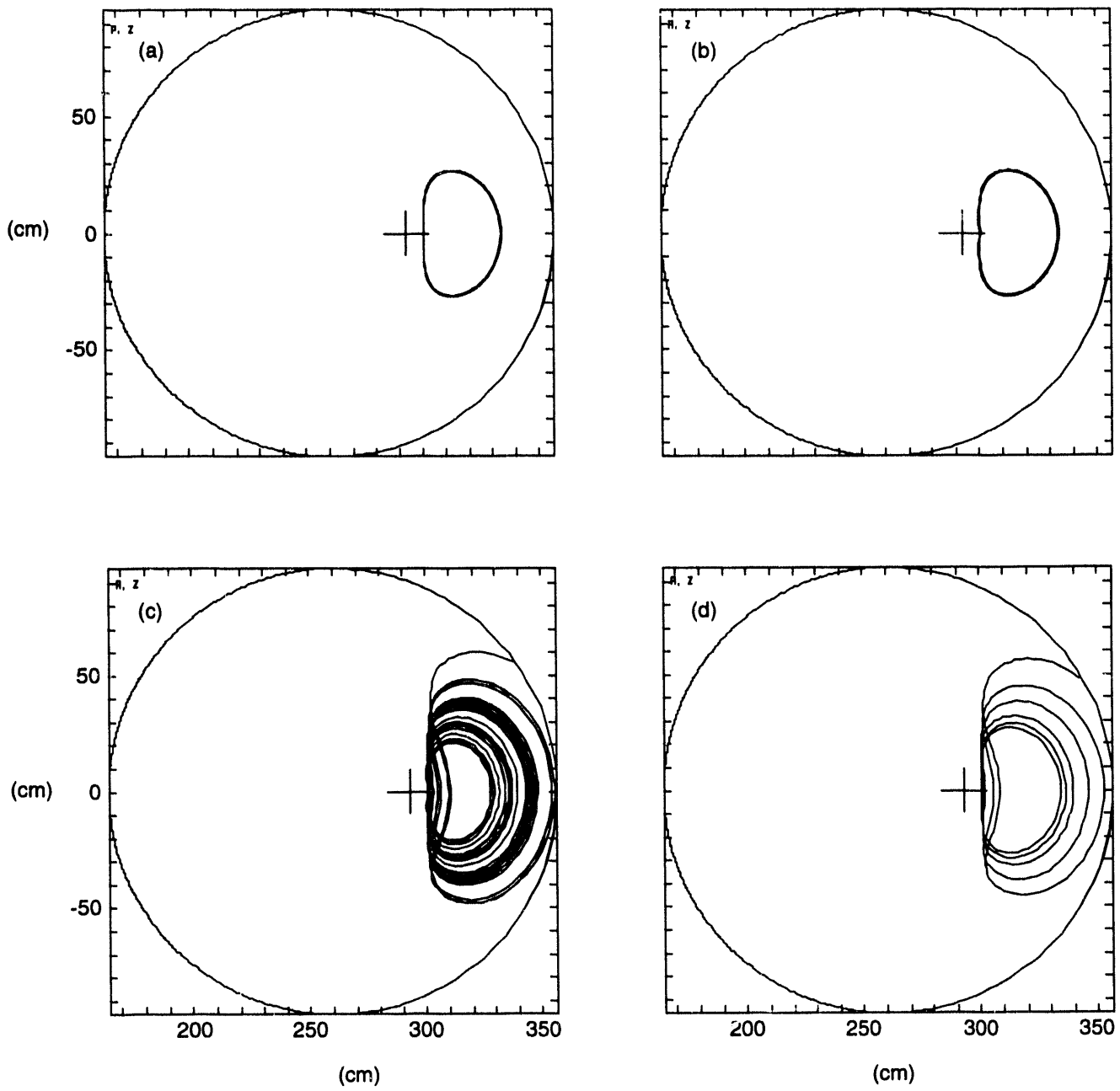

Fig. 8

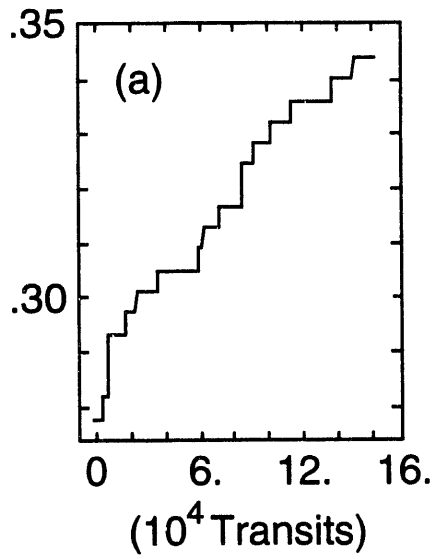
.35
(a)
.30
0
6.
12.
16.
(10^4 Transits)

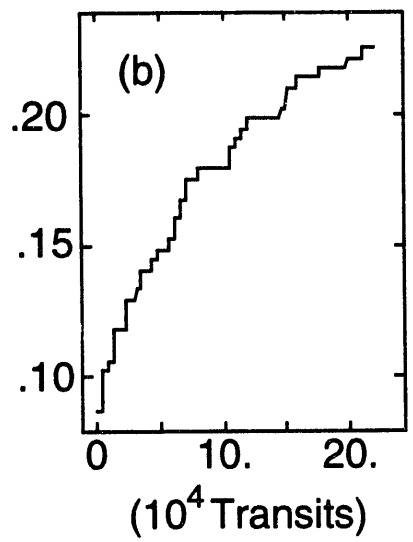
(b)
.20
.15
.10
0
10.
20.
(10^4 Transits)

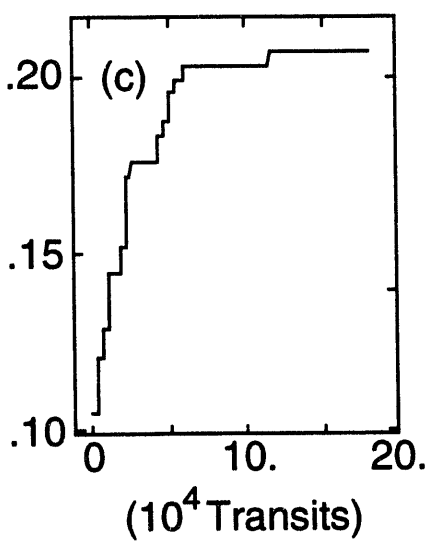
.20
(c)
.15
.10
0
10.
20.
(10^4 Transits)

Fig. 9

PPPL#94X0152

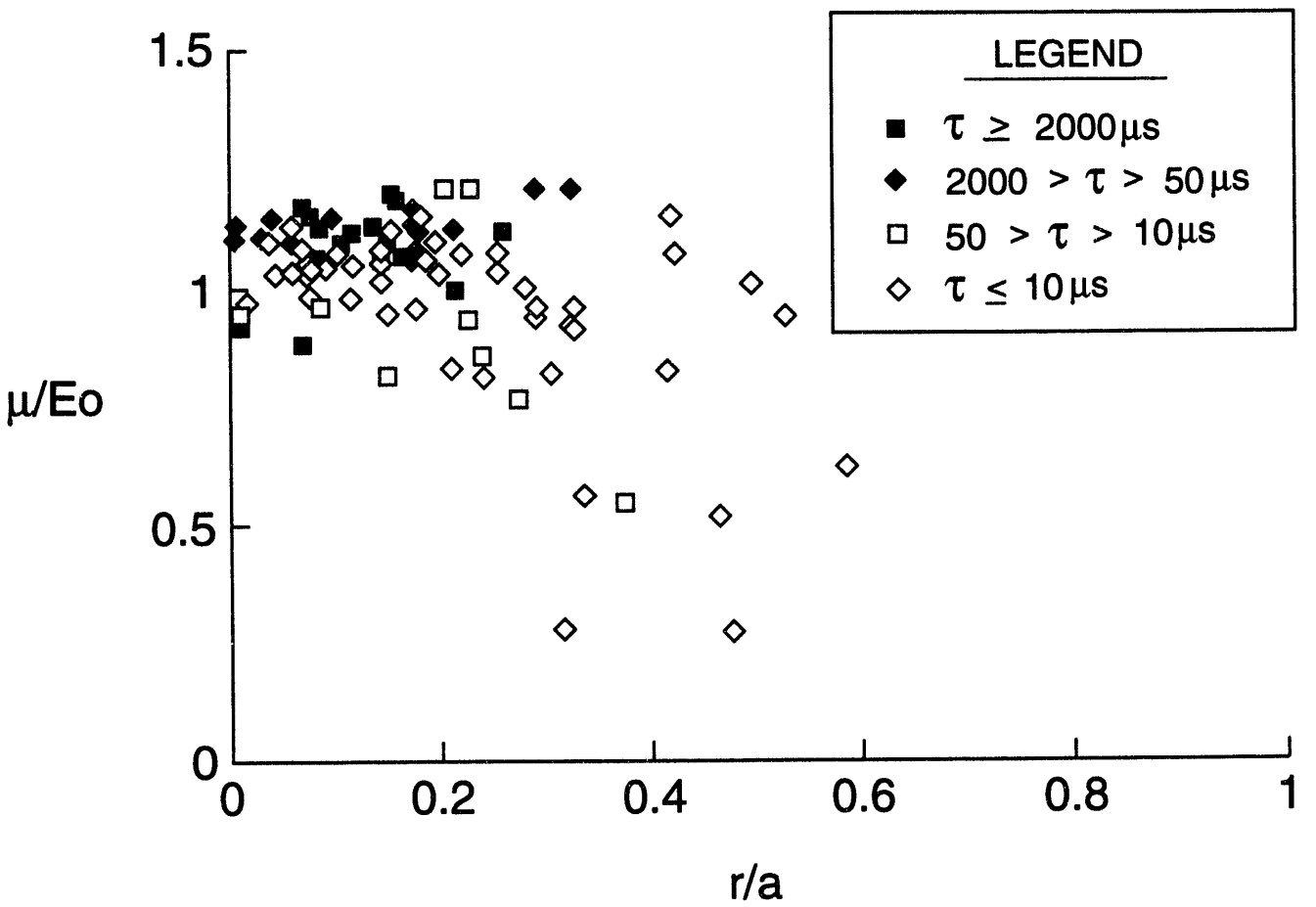

Fig. 10

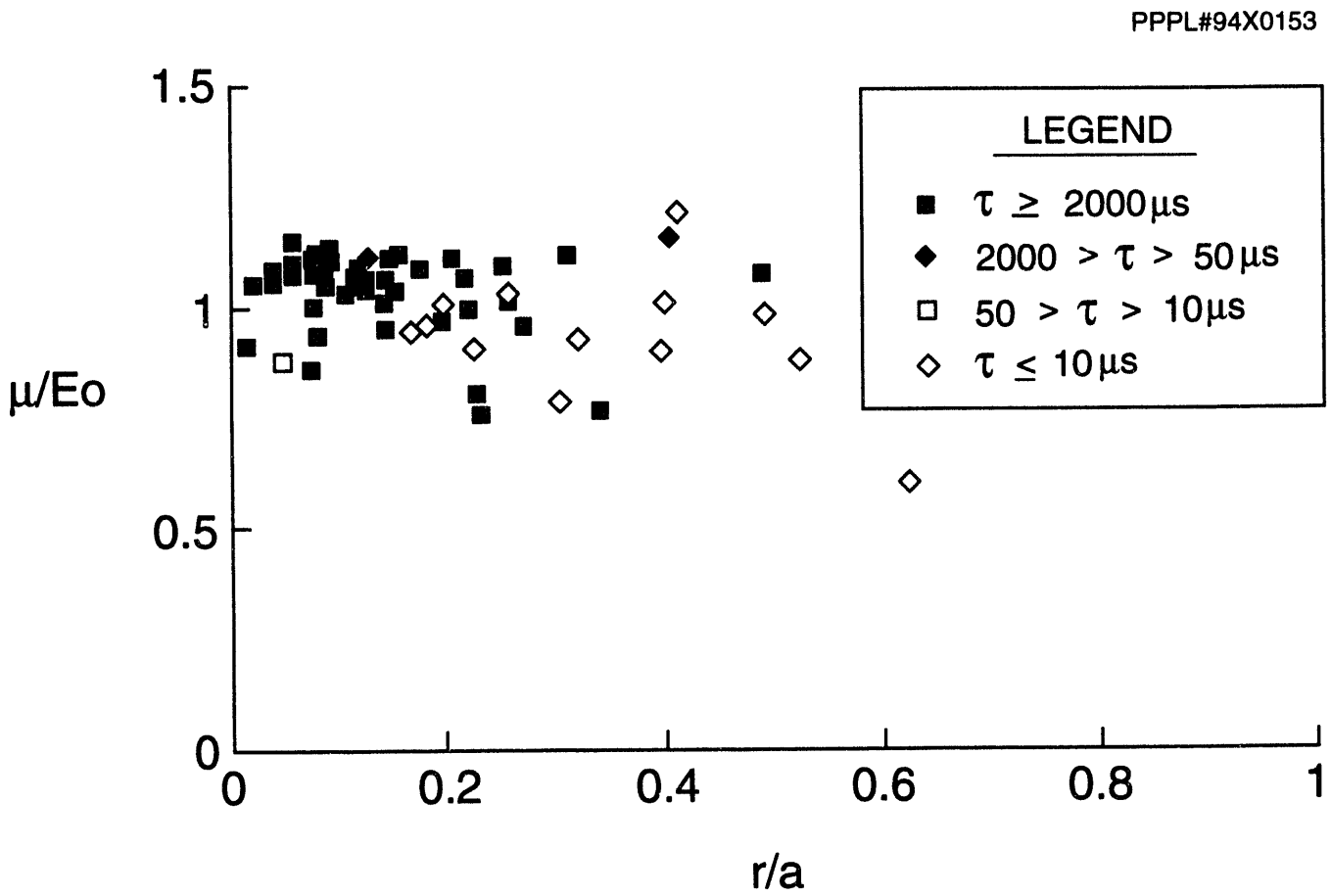
PPPL#94X0153
1.5
1
0.5
0
μ/Eo
0
0.2
0.4
0.6
0.8
1
r/a
LEGEND
τ ≥ 2000μs
2000 > τ > 50μs
50 > τ > 10μs
τ ≤ 10μs

Fig. 11

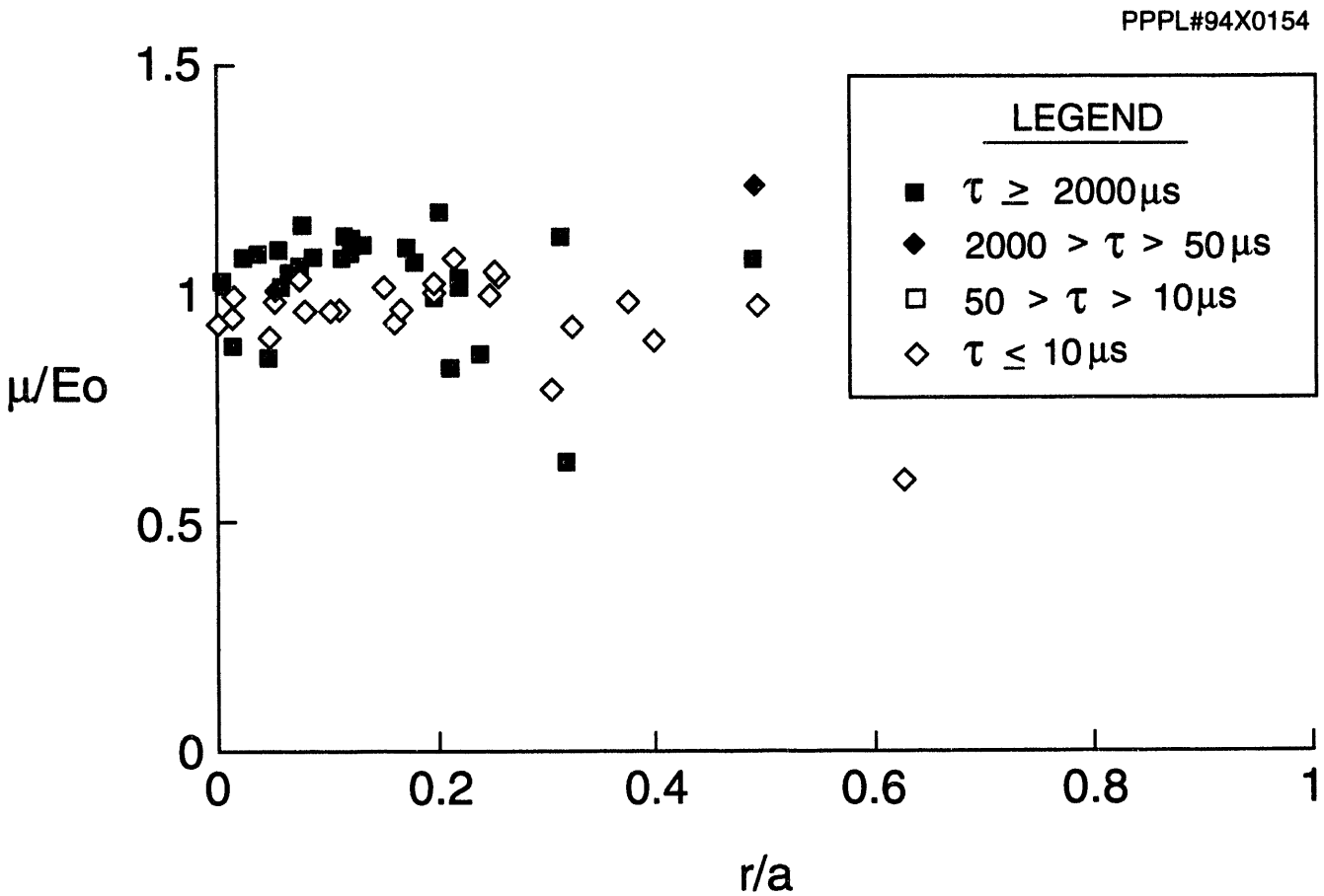
PPPL#94X0154
1.5
1
0.5
0
μ/Eo
0
0.2
0.4
0.6
0.8
1
r/a
LEGEND
τ ≥ 2000μs
2000 > τ > 50μs
50 > τ > 10μs
τ ≤ 10μs

Fig. 12

PPPL#94X0149

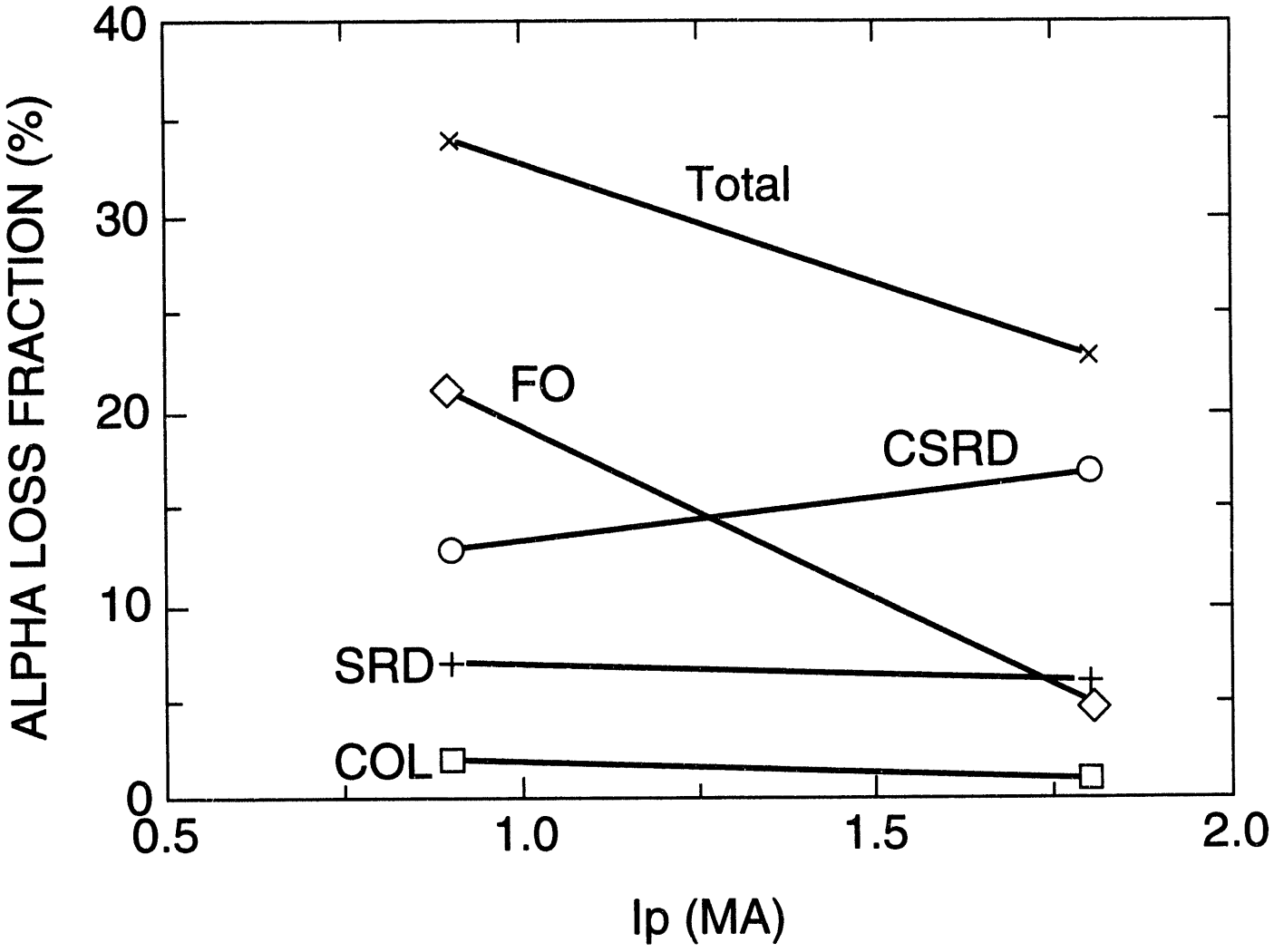

Fig. 13

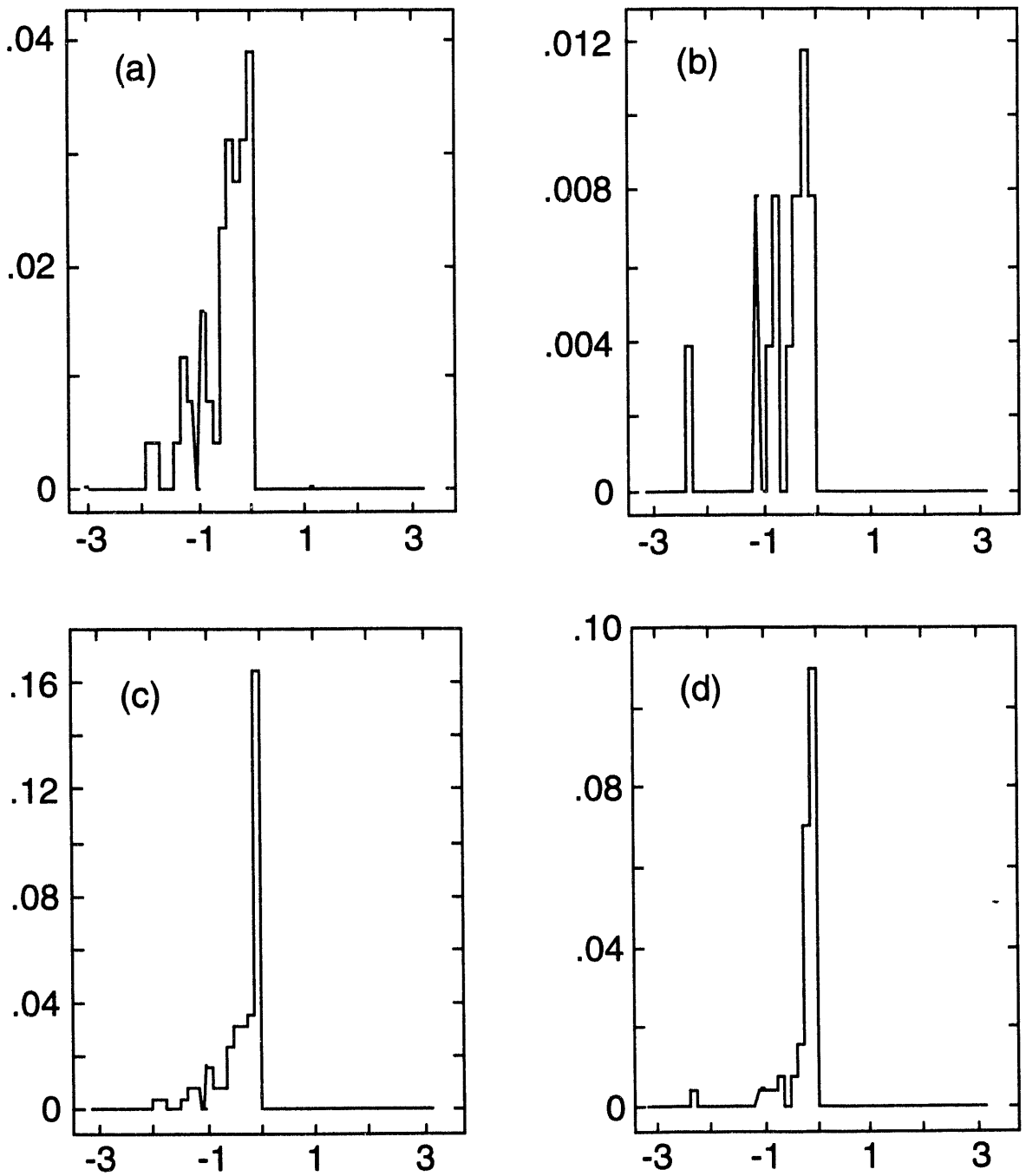
(a)
.04
.02
0
-3
-1
1
3
(b)
.012
.008
.004
0
-3
-1
1
3
(c)
.16
.12
.08
.04
0
-3
-1
1
3
(d)
.10
.08
.04
0
-3
-1
1
3

Fig. 14

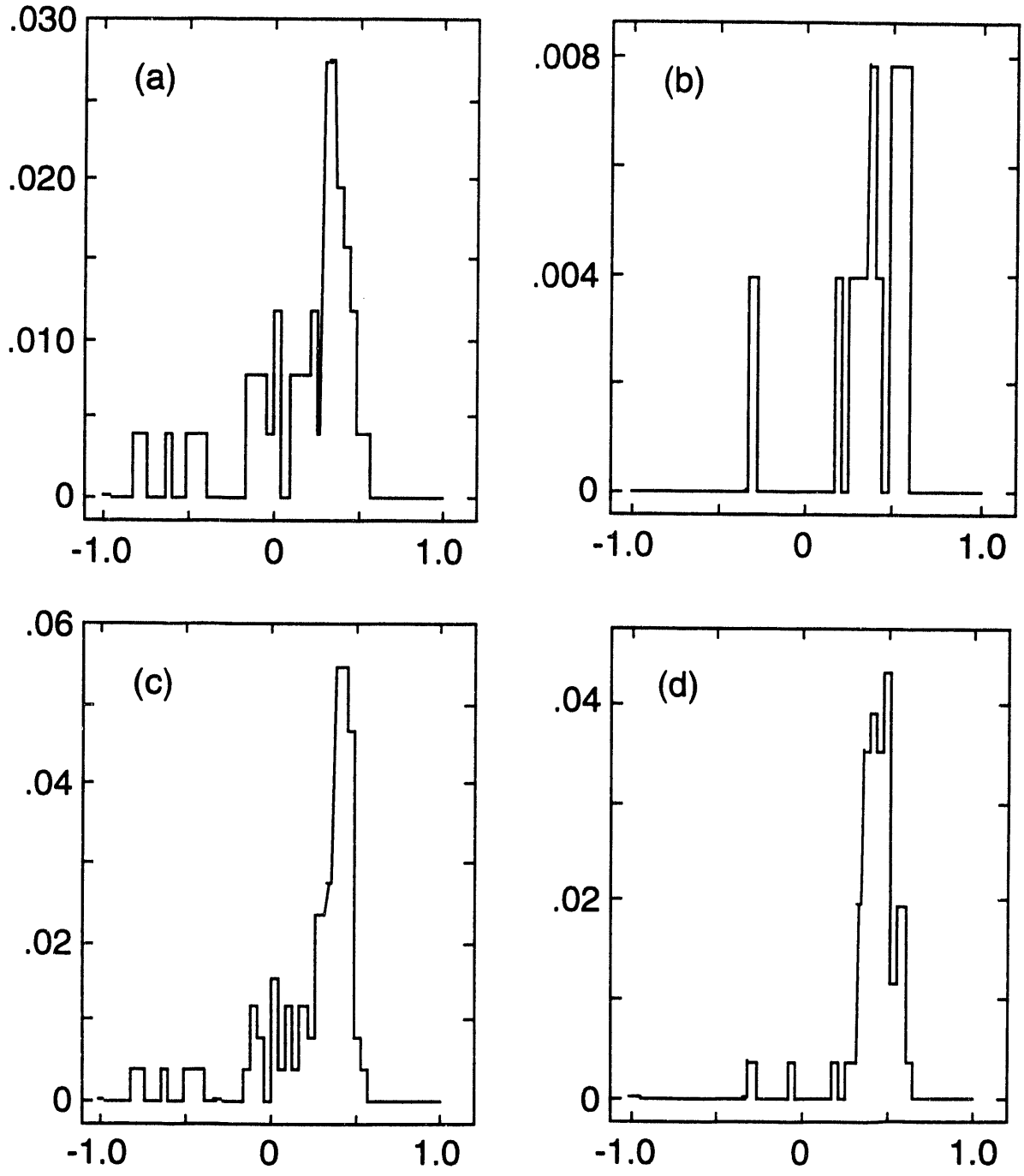
(a)
.030
.020
.010
0
-1.0
0
1.0
(b)
.008
.004
0
-1.0
0
1.0
(c)
.06
.04
.02
0
-1.0
0
1.0
(d)
.04
.02
0
-1.0
0
1.0

Fig. 15

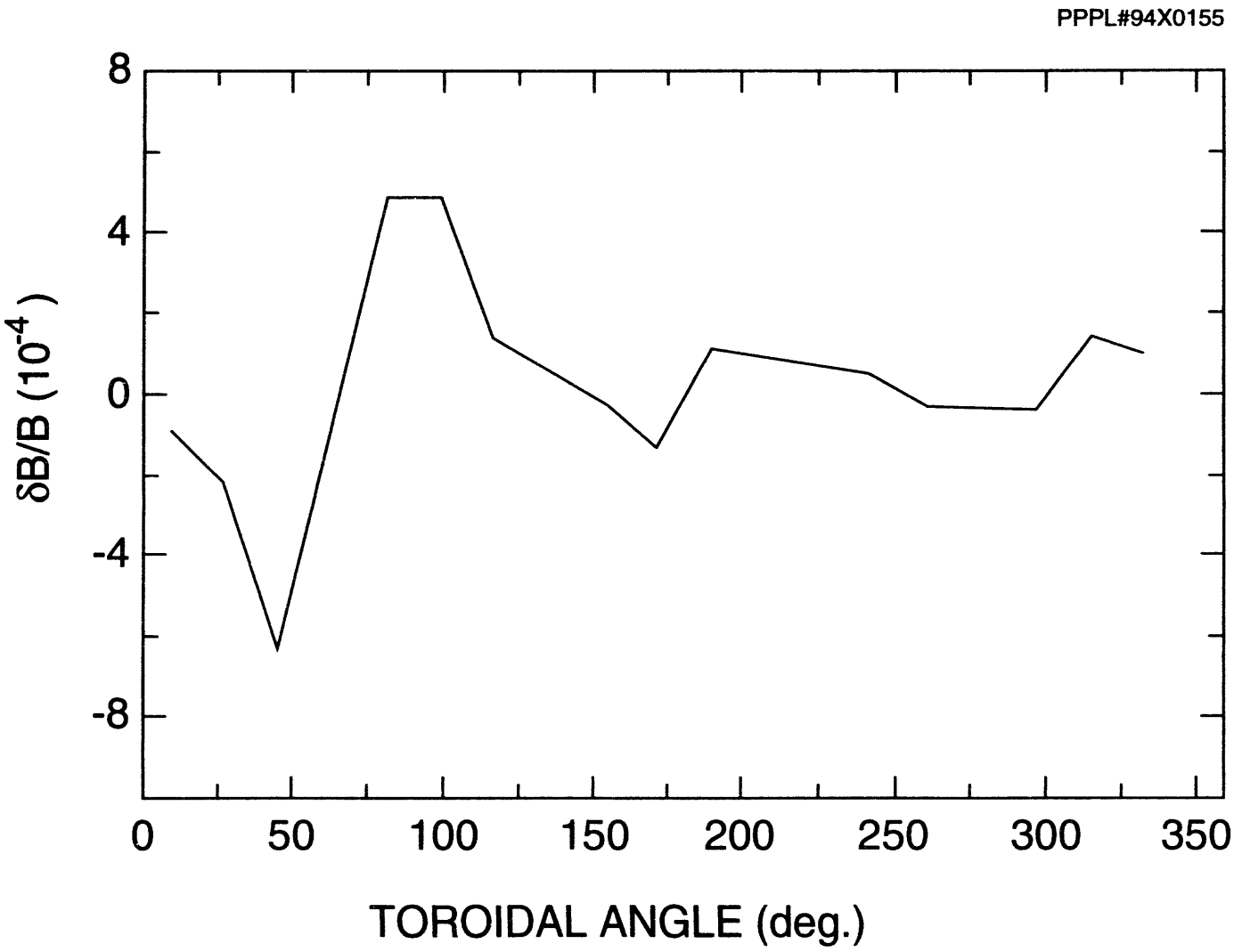
PPPL#94X0155
8
4
0
-4
-8
δB/B (10^-4)
0
50
100
150
200
250
300
350
TOROIDAL ANGLE (deg.)

Fig. 16

EXTERNAL DISTRIBUTION IN ADDITION TO UC-420

Dr. F. Paoloni, Univ. of Wollongong, AUSTRALIA
Prof. R.C. Cross, Univ. of Sydney, AUSTRALIA
Plasma Research Lab., Australian Nat. Univ., AUSTRALIA
Prof. I.R. Jones, Flinders Univ, AUSTRALIA
Prof. F. Cap, Inst. for Theoretical Physics, AUSTRIA
Prof. M. Heindler, Institut für Theoretische Physik, AUSTRIA
Prof. M. Goossens, Astronomisch Instituut, BELGIUM
Ecole Royale Militaire, Lab. de Phy. Plasmas, BELGIUM
Commission-European, DG. XII-Fusion Prog., BELGIUM
Prof. R. Bouciqué, Rijksuniversiteit Gent, BELGIUM
Dr. P.H. Sakanaka, Instituto Fisica, BRAZIL
Prof. Dr. I.C. Nascimento, Instituto Fisica, Sao Paulo, BRAZIL
Instituto Nacional De Pesquisas Espaciais-INPE, BRAZIL
Documents Office, Atomic Energy of Canada Ltd., CANADA
Ms. M. Morin, CCFM/Tokamak de Varennes, CANADA
Dr. M.P. Bachynski, MPB Technologies, Inc., CANADA
Dr. H.M. Skarsgard, Univ. of Saskatchewan, CANADA
Prof. J. Teichmann, Univ. of Montreal, CANADA
Prof. S.R. Sreenivasan, Univ. of Calgary, CANADA
Prof. T.W. Johnston, INRS-Energie, CANADA
Dr. R. Bolton, Centre canadien de fusion magnétique, CANADA
Dr. C.R. James,, Univ. of Alberta, CANADA
Dr. P. Lukác, Komenského Universzita, CZECHO-SLOVAKIA
The Librarian, Culham Laboratory, ENGLAND
Library, R61, Rutherford Appleton Laboratory, ENGLAND
Mrs. S.A. Hutchinson, JET Library, ENGLAND
Dr. S.C. Sharma, Univ. of South Pacific, FIJI ISLANDS
P. Mähönen, Univ. of Helsinki, FINLAND
Prof. M.N. Bussac, Ecole Polytechnique,, FRANCE
C. Mouttet, Lab. de Physique des Milieux Ionisés, FRANCE
J. Radet, CEN/CADARACHE - Bat 506, FRANCE
Prof. E. Economou, Univ. of Crete, GREECE
Ms. C. Rinni, Univ. of Ioannina, GREECE
Preprint Library, Hungarian Academy of Sci., HUNGARY
Dr. B. DasGupta, Saha Inst. of Nuclear Physics, INDIA
Dr. P. Kaw, Inst. for Plasma Research, INDIA
Dr. P. Rosenau, Israel Inst. of Technology, ISRAEL
Librarian, International Center for Theo Physics, ITALY
Miss C. De Palo, Associazione EURATOM-ENEA , ITALY
Dr. G. Grosso, Istituto di Fisica del Plasma, ITALY
Prof. G. Rostangni, Istituto Gas Ionizzati Del Cnr, ITALY
Dr. H. Yamato, Toshiba Res & Devel Center, JAPAN
Prof. I. Kawakami, Hiroshima Univ., JAPAN
Prof. K. Nishikawa, Hiroshima Univ., JAPAN
Librarian, Naka Fusion Research Establishment, JAERI, JAPAN
Director, Japan Atomic Energy Research Inst., JAPAN
Prof. S. Itoh, Kyushu Univ., JAPAN
Research Info. Ctr., National Instit. for Fusion Science, JAPAN
Prof. S. Tanaka, Kyoto Univ., JAPAN
Library, Kyoto Univ., JAPAN
Prof. N. Inoue, Univ. of Tokyo, JAPAN
Secretary, Plasma Section, Electrotechnical Lab., JAPAN
Dr. O. Mitarai, Kumamoto Inst. of Technology, JAPAN
Dr. G.S. Lee, Korea Basic Sci. Ctr., KOREA
J. Hyeon-Sook, Korea Atomic Energy Research Inst., KOREA
D.I. Choi, The Korea Adv. Inst. of Sci. & Tech., KOREA
Prof. B.S. Liley, Univ. of Waikato, NEW ZEALAND
Inst of Physics, Chinese Acad Sci PEOPLE'S REP. OF CHINA
Library, Inst. of Plasma Physics, PEOPLE'S REP. OF CHINA
Tsinghua Univ. Library, PEOPLE'S REPUBLIC OF CHINA
Z. Li, S.W. Inst Physics, PEOPLE'S REPUBLIC OF CHINA
Prof. J.A.C. Cabral, Instituto Superior Tecnico, PORTUGAL
Prof. M.A. Hellberg, Univ. of Natal, S. AFRICA
Prof. D.E. Kim, Pohang Inst. of Sci. & Tech., SO. KOREA
Prof. C.I.E.M.A.T, Fusion Division Library, SPAIN
Dr. L. Stenflo, Univ. of UMEA, SWEDEN
Library, Royal Inst. of Technology, SWEDEN
Prof. H. Wilhelmson, Chalmers Univ. of Tech., SWEDEN
Centre Phys. Des Plasmas, Ecole Polytech, SWITZERLAND
Bibliotheek, Inst. Voor Plasma-Fysica, THE NETHERLANDS
Asst. Prof. Dr. S. Cakir, Middle East Tech. Univ., TURKEY
Dr. V.A. Glukhikh,Sci. Res. Inst. Electrophys.I Apparatus, USSR
Dr. D.D. Ryutov, Siberian Branch of Academy of Sci., USSR
Dr. G.A. Eliseev, I.V. Kurchatov Inst., USSR
Librarian, The Ukr.SSR Academy of Sciences, USSR
Dr. L.M. Kovrizhnykh, Inst. of General Physics, USSR
Kernforschungsanlage GmbH, Zentralbibliothek, W. GERMANY
Bibliothek, Inst. Für Plasmaforschung, W. GERMANY
Prof. K. Schindler, Ruhr-Universität Bochum, W. GERMANY
Dr. F. Wagner, (ASDEX), Max-Planck-Institut, W. GERMANY
Librarian, Max-Planck-Institut, W. GERMANY

DATE
FILMED
10/18/94

END